Non-Classical States of Matter in Spinor Bose-Einstein Condensates

---

Von der QUEST-Leibniz-Forschungsschule der
Gottfried Wilhelm Leibniz Universität Hannover

zur Erlangung des Grades

Doktor der Naturwissenschaften
- Dr. rer. nat. -

genehmigte Dissertation von

Dipl.-Phys. **Jan Christopher Peise**,
geboren am 21. Mai 1985 in Hannover

2015

Referent:	Prof. Dr. Wolfgang Ertmer, Institut für Quantenoptik, Hannover
Korreferent:	PD Dr. Carsten Klempt, Institut für Quantenoptik, Hannover
Korreferent:	Prof. Dr. Jan Arlt, Department of Physics and Astronomy, Aarhus

Tag der Promotion: 31. Juli 2015

Abstract

Quantum mechanics is one of the best tested theories of modern physics. The intriguing features of the quantum-mechanical microcosm are in strong contrast to our experience of the macroscopic world. However, the transition between these two worlds is not completely understood. Therefore, the validity of quantum mechanics needs to be tested with ever larger quantum systems. Quantum mechanics allows for a large variety of quantum technologies, whose performance increases with the size of the system. A prerequisite for many of these technologies is entanglement, a concept which lies at the heart of quantum mechanics. Thus, the generation of large entangled ensembles constitutes an important goal to test the validity of quantum mechanics and to explore the available tools for quantum information and metrology.

In this thesis, we employ spin-changing collisions in a ^{87}Rb Bose-Einstein condensate to generate entangled states of matter. Interparticle collisions transfer atoms from the initial Zeeman level $m_F = 0$ to $m_F = \pm 1$. Thereby, highly entangled ensembles of up to $10,000$ particles are created. We utilize this access to entanglement to investigate three important aspects of quantum theory with ultracold atoms. First, we realize a proof-of-principle experiment demonstrating an interferometric sensitivity of 1.6 dB below the standard quantum limit. We verify an entanglement of more than 68 particles. Second, Einstein-Podolsky-Rosen (EPR) correlations are realized. By applying an unbalanced homodyne detection for atoms, we fulfill the criterion for EPR correlations with a significance of 2.4 standard deviations. This constitutes the first demonstration of EPR correlations with massive particles. Third, the quantum Zeno effect (QZE) is used to suppress the transfer of atoms from $m_F = 0$ to $m_F = \pm 1$. The observed suppression is the first realization of the QZE in an unstable system with an indirect measurement. Furthermore, we discriminate between zero and few atoms in $m_F = +1$ to realize the first interaction-free measurement with ultracold atoms. We obtain an efficiency of 65 % for the interaction-free measurement. In summary, our results show a new method to create entangled states of matter to outperform the precision of classical interferometry and open a path for novel tests of quantum mechanics with an increasing system size.

Keywords: Bose-Einstein condensate, spin dynamics, entanglement, Einstein-Podolsky-Rosen correlation, quantum Zeno effect, interaction-free measurements

Zusammenfassung

Die Quantenmechanik ist eine der am besten getesteten Theorien der modernen Physik. Die faszinierenden Eigenschaften des quantenmechanischen Mikrokosmos stehen in starkem Kontrast zu unserer Alltagserfahrung aus der makroskopischen Welt. Der Übergang zwischen diesen Welten ist allerdings noch nicht vollständig verstanden. Deshalb wird die Gültigkeit der Quantenmechanik mit immer größeren Quantensystemen getestet. Die Quantenmechanik ermöglicht eine Vielfalt an Quantentechnologien, deren Leistungsfähigkeit mit zunehmender Systemgröße steigt. Eine Grundvoraussetzung für viele dieser Technologien ist Verschränkung, ein Konzept, das untrennbar mit der Quantenmechanik verbunden ist. Daher stellt die Erzeugung großer verschränkter Ensembles ein wichtiges Ziel dar, um die Gültigkeit der Quantenmechanik zu testen und die möglichen Werkzeuge der Quantentechnologie und Quantenmetrologie zu erforschen.

Im Rahmen dieser Arbeit werden spinändernde Stöße in ^{87}Rb Bose-Einstein-Kondensaten genutzt, um verschränkte Zustände mit Materie zu erzeugen. Interatomare Kollisionen transferieren Atome aus dem anfänglichen Zeeman-Zustand $m_F = 0$ nach $m_F = \pm 1$. Dabei entstehen hochgradig verschränkte Ensembles mit bis zu 10.000 Teilchen. Wir verwenden diesen Zugang zu verschränkten Ensembles um drei wichtige Aspekte der Quantentheorie mit ultrakalten Atomen zu untersuchen. Zuerst zeigen wir in einem Machbarkeitsexperiment, dass Atominterferometrie jenseits des Standard-Quanten-Limits (SQL) möglich ist und demonstrieren eine Sensitivität von 1,6 dB unterhalb des SQL. Wir bestimmen eine Verschränkung von mindestens 68 Teilchen. Zweitens realisieren wir Einstein-Podolsky-Rosen-Korrelationen (EPR-Korrelationen). Indem eine asymmetrische Homodyn-Detektion für Atome realisiert wird, ist es uns möglich das Kriterium für EPR-Korrelationen mit einer Signifikanz von 2,4 Standardabweichungen zu erfüllen. Dies ist die erste Demonstration von EPR-Korrelationen mit massebehafteten Teilchen. Drittens zeigen wir, dass der Quanten-Zeno-Effekt (QZE) benutzt werden kann, um den Transfer von $m_F = 0$ nach $m_F = \pm 1$ zu unterbinden. Die beobachtete Unterdrückung stellt die erste Realisierung des QZE in instabilen Systemen mit einer indirekten Messung dar. Des Weiteren unterscheiden wir zwischen null und wenigen Teilchen in $m_F = +1$ und realisieren damit die erste wechselwirkungsfreie Quantenmessung mit Atomen. Wir bestimmen eine Effizienz von 65 %. Zusammenfassend zeigen die Ergebnisse eine neue Methode zur Erzeugung verschränkter Zustände mit Materie auf. Sie ermöglicht die Verbesserung der Präzision von klassischen Atominterferometern und eröffnet neue Wege um Tests der Quantenmechanik mit immer größeren Systemen durchzuführen.

Schlagwörter: Bose-Einstein-Kondensat, Spindynamik, Verschränkung, Einstein-Podolsky-Rosen-Korrelationen, Quanten-Zeno-Effekt, wechselwirkungsfreie Quantenmessungen

Contents

1 Introduction **1**

2 Creation, application and quantification of entanglement in spinor Bose-Einstein condensates **7**
2.1 Spin-changing collisions in a Bose-Einstein condensate 7
2.2 Spontaneous symmetry breaking in spinor Bose-Einstein condensates . . 10
2.3 Non-classical atom interferometry 11
2.4 Entanglement quantification of Dicke states 13
2.5 Verifying metrological usefulness of Dicke states 14

3 Einstein-Podolsky-Rosen correlations with massive particles **15**
3.1 The Einstein-Podolsky-Rosen thought experiment 15
3.2 Experimental realizations 18
3.3 First demonstration of Einstein-Podolsky-Rosen correlations with massive particles 19

4 Quantum Zeno suppression of spin dynamics and interaction-free measurements **21**
4.1 The quantum Zeno effect 21
4.2 Interaction-free measurements 23
4.3 Multi-particle interaction-free measurements with atoms by quantum Zeno suppression 25

5 Outlook **29**

Bibliography **30**

Publications **41**

1 Introduction

Interferometers are among the most precise measurement devices. They rely on interference and therefore on the wave nature of particles. Interferometers with light are commonly used for gyroscopes employed for navigation in planes. More advanced light-based interferometers are employed to measure the earth's rotation [1] and search for gravitational waves [2, 3]. On the other hand, interferometers with massive particles enable to measure quantities like magnetic field [4] or gravity [5]. Furthermore, fountain clocks utilize interferometers with ultracold atoms based on hyperfine transitions to define the second [6]. In the future, they might be replaced by more precise clocks based on optical transitions in neutral atoms [7] or ions [8]. In addition, these clocks allow to test the variation of fundamental constants [9]. On the other hand, compact microwave clocks allow for the precise determination of position via the *Global Positioning System* (GPS).

However, even without technical noise, the precision of these devices is limited by quantum mechanics. After a particle passes an interferometer, it is in a superposition of being in both output ports. The signal is encoded in the probabilities for each port. The measurement at the output ports forces the particle to localize in either one of the ports, and the granular particle nature becomes visible. Consequently, many particles have to pass the interferometer in order to determine these probabilities. This can be carried out successively or simultaneously. If the particles are uncorrelated, the precision is limited by shot noise, which is given by $1/\sqrt{N}$ for a single measurement, where N denotes the number of particles. The shot noise limit can be surpassed if the interferometer operates with entangled particles. These quantum mechanical correlations allow to operate at the Heisenberg limit, given by $1/N$.

Besides precision interferometry, the performance of many other quantum technologies critically depends on the achievable degree of multi-particle entanglement. Entanglement constitutes a characteristic feature of quantum mechanics. The intriguing correlations seem to only appear in the microscopic world. In the macroscopic world, these correlations have never been observed. The boundary between these two worlds is not fully understood. Entanglement results in features of particles which are beyond our everyday experience. For example, quantum mechanics predicts that one particle of an entangled pair, which is spatially separated, depends on what measurement is carried out on the other particle. Hence, one particle can *steer* [10] the other. When this *"spooky action at a distance"* (as called by A. Einstein) became apparent, an intense debate started whether quantum mechanics is adequate. Among the critics, A. Einstein argued that it has to be considered incomplete [11], whereas E. Schrödinger doubted its validity for spatially separated systems [12]. However, experiments confirm quantum mechanics to be correct and complete as far as it is experimentally accessible. Most tests have uti-

lized few photons and ions. To verify quantum mechanics with large entangled ensembles ultracold atoms are a suitable candidate. They provide various mechanisms to create entanglement.

The generation of entangled states with neutral atoms is divided in two types. (i) Entanglement by atom-light interaction and (ii) entanglement by collisions. The former was demonstrated with vapor cells at room temperature [13] and with laser cooled ensembles [14–17]. The latter is based on the precise control of collisions in Bose-Einstein condensates (BECs). The arising nonlinear interaction can generate entanglement in the external degree of freedom [18, 19] as well as in the spin degree of freedom [20, 21]. This thesis is centered around the generation of entangled states via spin-changing collisions. This phenomenon is equivalent to *optical parametric-down conversion*. It is a common technique to generate entangled states of light. Here, photons of a strong pump field can decay in a nonlinear crystal, generating pairs of photons at half the energy. These so-called *signal* and *idler* modes are highly entangled. In atom optics, a spinor BEC initially prepared in the $m_F = 0$ state replaces the pump field. The state decays by means of collisions, producing pairs of atoms in $m_F = \pm 1$, which correspond to the signal and idler modes and exhibit strong quantum-mechanical correlations.

Spin dynamics constitutes an important tool to access the fascinating phenomena and applications of entangled many-particle states in the field of atom optics. In this work, spin dynamics is used as a source of non-classical states of matter to perform quantum optics experiments along three directions: This thesis demonstrates a proof-of-principle experiment of (i) quantum-enhanced atom interferometry, as well as a fundamental test of quantum mechanics by the demonstration of (ii) Einstein-Podolsky-Rosen correlations and the first realization of a (iii) high-efficiency interaction-free measurements with atoms based on the quantum Zeno effect.

Quantum-enhanced atom interferometry

In order to perform atom interferometry beyond the standard quantum limit, methods to prepare and quantify entangled states are needed. The most prominent example of non-classical states of matter are so-called spin-squeezed states. They can be generated by controlled interparticle interactions in BECs. This was demonstrated in Ref. [20]. Here, the *one-axis twisting scheme* as proposed in Ref. [22] was implemented for the realization of a non-classical beam splitter. It allowed to generate a squeezed phase uncertainty at the expense of an increased population imbalance uncertainty. The accumulated phase during the subsequent evolution was resolved with an improved sensitivity compared to a coherent spin state. A second, classical beam splitter converted the accumulated phase into a population imbalance. The sensitivity surpassed the standard quantum limit by 15 %. A criterion for the determination of the entanglement depth [23] revealed a depth of 170 atoms. Even an on-chip realization with spin-squeezed states in a full Mach-Zehnder interferometer has been demonstrated [19] with an entanglement depth of 150 atoms.

In contrast to spin squeezing, we utilize spin dynamics and generate Dicke-like states. In chapter 2, we demonstrate an interferometric sensitivity of 1.6 dB below the standard

quantum limit. To characterize the entanglement depth of our state we developed a new criterion. We obtain an entanglement depth of 68 particles.

Einstein-Podolsky-Rosen correlations

Quantum mechanics predicts a phenomenon termed *steering* by E. Schrödinger [10]. It constitutes the failure of local realism in quantum mechanics, which is revealed in the Einstein-Podolsky-Rosen (EPR) paradox [11], published in 1935. In the EPR thought experiment, two entangled particles originate from a common source and fly apart. They are perfectly correlated in position and perfectly anti-correlated in momentum. Even though the particles are spatially separated, their quantum-mechanical state is inseparable due to the correlations. According to quantum mechanics, a measurement of one particle's position or momentum will immediately influence the other particle. Thus, the second particle is either steered [10, 12] by the measurement and local realism does not hold or quantum mechanics is incomplete. EPR speculated that the latter is correct and that it is possible to complement quantum mechanics with *local* hidden variables, such that steering does not occur. In 1952, D. Bohm proved that a *nonlocal* hidden variable theory is consistent with quantum mechanics [24], however, J. Bell could show that a *local* hidden variable theory is incompatible with quantum mechanics [25].

Since experiments always include noise, the perfect correlations implied by EPR are experimentally not possible. Therefore, M. Reid introduced a criterion [26] that accounts for noise. The criterion is an inferred Heisenberg uncertainty, whose violation constitutes a demonstration of the EPR paradox. Here, field quadratures are measured in order to demonstrate the paradox. In 1992, Ou et. al. [27] realized such a violation based on the signal and idler modes generated by optical parametric down-conversion. These modes were spatially separated and analyzed via homodyne detection. Numerous realizations followed based on photons. However, massive particles may be more strictly bound to the concept of local realism compared to fields [28] and a verification with massive particles presents an important step. Previous experiments demonstrated a weaker inseparability criterion [29, 30] based on entanglement by atom-light interaction [31] in vapor cells at room temperature and by spin-changing collisions in BECs [32]. However, they could not confirm the strong correlations needed for a realization of the EPR paradox.

In chapter 3, we utilize spin dynamics to generate a two-mode squeezed vacuum and show the strong correlations needed for the EPR paradox. The created state is analysed via an unbalanced homodyne detection for atoms. We measure a variance product of 0.18, which is below the threshold of 1/4 with a significance of 2.4 standard deviations. It is the first demonstration of EPR correlations with massive particles.

High-efficiency interaction-free measurements based on the quantum Zeno effect

A remarkable feature of quantum mechanics occurs if a system is repeatedly measured. This was investigated by B. Misra and E. Sudarshan [33] in 1977. They considered an unstable particle under frequent observation. If the system has only a short time to decay until it is measured, it is likely that the particle's state is projected back onto the

initial (undecayed) state. If the measurement is frequent enough, the particle will never decay. The impossibility of evolution of an object under observation resembles one of the paradoxes by the Greek philosopher Zeno, hence, this quantum phenomenon was named quantum Zeno effect (QZE). Ultracold atoms form an excellent test bed, since measurements by laser light are well controlled and unstable systems are accessible in various ways. Either the instability can be simulated with stable systems or a truly unstable systems is employed which behavior can be tailored. For example, a simulated instability was applied to cold ions [34] and BECs [35]. In Ref. [35], the first quantitative comparison between repeated and continuous measurements was performed. A truly spontaneous decay was investigated in an accelerated optical lattice [36]. The authors also demonstrated the anti-Zeno effect, where the decay is accelerated by measurements. The QZE also allows to restrict the evolution of a quantum system to a small subspace [37], as predicted in Ref. [38]. This enables a very important application of the QZE, because it can increase the coherence time in the presence of a decay channel. Furthermore, the QZE is suitable to protect entanglement [39], although the Zeno protection becomes more challenging for non-classical states [40].

The quantum Zeno suppression also allows for high-efficiency *interaction-free measurements* (IFMs). The concept of IFMs was introduced by A. Elitzur and L. Vaidman [41] in 1993. IFMs allow to ascertain the presence of an object without interacting with it. The basic idea utilizes the nonlocality of a single photon in a Mach-Zehnder interferometer. Additionally, a classical object whose presence shall be detected is placed in one of the interferometer arms. Due to the object, the interference at the output of the Mach-Zehnder interferometer does not take place, witnessing the presence of the object, even if the photon is not absorbed by the object. This detection scheme is also called *quantum interrogation*.

The highest efficiency of an interaction-free detection possible within the described setup is $\eta_{\mathrm{IFM}} = 50\,\%$. It can be increased to $100\,\%$ if the technique is combined with the QZE. The realization of a high-efficiency IFM based on the QZE was recognized and experimentally verified with photons by P. Kwiat and colleagues [42, 43]. IFMs provide quantum techniques like all optical switching [44] and counterfactual quantum computation [45]. Furthermore, it is proposed to eliminate the sample damage in electron microscopy [46].

In chapter 4, we demonstrate for the first time the indirect, negative-result QZE in a truly unstable system. Furthermore, the first demonstration of an IFM with ultracold atoms is reported. It is implemented by the described realization of the quantum Zeno effect in spin dynamics. We obtain an efficiency of $\eta_{\mathrm{IFM}} = 65\,\%$ of the interaction-free detection. This multi-particle realization of an interaction-free measurement is only weakly affected by losses and decoherence.

This thesis is organized as follows: In chapter 2, we start with a brief introduction to the relevant properties of spin dynamics in BECs. Afterwards, the mechanism of spontaneous symmetry breaking is discussed and an interferometric sensitivity beyond

the standard quantum limit is presented. We close this chapter with the verification of multi-particle entanglement and a simplified procedure how to determine the metrological usefulness based on collective measurements. In chapter 3, the original EPR paradox is discussed and EPR correlations with massive particles are demonstrated. In chapter 4, we begin with the fundamentals of the QZE. We present the first indirect, negative-result QZE in an unstable system. Subsequent, the concept of IFMs and the extensions to high-efficiency IFMs by QZE is introduced. The chapter is completed with the first realization of an IFM with ultracold atoms. We complete with an outlook in chapter 5.

2 Creation, application and quantification of entanglement in spinor Bose-Einstein condensates

A source of entanglement is a basic prerequisite for many applications in the field of quantum technology. To utilize such technologies, a well understood experimental procedure creating entanglement is vital. This work is centered around such a mechanism, namely the generation of multi-particle entanglement in a BEC by means of spin-changing collisions. Therefore, section 2.1 starts with the fundamentals of spin dynamics and section 2.2 shows the spontaneous symmetry breaking spin dynamics exhibits. In section 2.3 quantum-enhanced metrology based on spin-changing collisions is demonstrated, which is an indirect proof of entanglement. Furthermore, the amount of multi-particle entanglement is determined in section 2.4. Section 2.5 completes this chapter by presenting a general method that allows for the determination of the metrological usefulness of the created states without executing the metrological task.

2.1 Spin-changing collisions in a Bose-Einstein condensate

The first observations of Bose-Einstein condensation in the groups of C. Wieman and W. Ketterle [47, 48] in 1995 were achieved with atoms in magnetic traps. Consequently, the internal spin degree of freedom was restricted to those spin states which are trapped due to their low-field seeking behavior. Three years later, the first BEC in an optical dipole trap was demonstrated [49] in which all magnetic sublevels can be trapped equally. In such a trap, a BEC can have several spin components which can interact with each other. The resulting temporal evolution can become very complex, leading to many-particle entangled states or spatial structures which break the symmetry of the system. A comprehensive review which includes a basic theoretical description of spinor BECs can be found in Refs. [50, 51].

This thesis focuses on spin-changing collisions in a ^{87}Rb BEC confined in a crossed-beam dipole trap. The two hyperfine ground states $F = 1$ and $F = 2$ of ^{87}Rb have $2F+1$ Zeeman sublevels labeled m_F. This single-particle description breaks down if two particles approach each other. At small distances, the atoms may enter a collision channel of their molecular potential which can mix the different Zeeman sublevels. Therefore, the spin of the output states can change compared to the initial states. Such collisions can

also change the hyperfine state of the atoms from $F = 2$ to $F = 1$. This releases a large amount of kinetic energy, expelling the atoms from the trap. The resulting loss mechanism is small on the time scale of our experiment. Neglecting this small loss term, we restrict the description to the case where the hyperfine states of input and output state are equal. Due to the ultracold temperature of the condensate, only s-wave scattering is allowed which means that the total angular momentum is conserved. Thus, the spin projection of input and output states must be preserved as well, consequently

$$^{\text{in}}m_F + ^{\text{in}}m'_F = ^{\text{out}}m_F + ^{\text{out}}m'_F \tag{2.1}$$

has to be fulfilled. Starting from a spin-polarized BEC in $m_F = 0$, spin dynamics transfers atoms in pairs to $m_F = \pm 1$. In the $F = 2$ manifold, a transfer to $m_F = \pm 2$ is allowed in principle but the time scale is much longer than the transfer to $m_F = \pm 1$. Therefore, it can be neglected. In the following, we consider the case where the number of atoms which are transferred to $m_F = \pm 1$ are small compared to the initial condensate. For negligible depletion of the initial condensate, the condensate can be treated as a classical field. Thus, the creation and annihilation operators for $m_F = 0$ can be replaced by complex numbers. This approach is called the parametric approximation. Within these assumptions, the process of spin dynamics resembles *spontaneous parametric down-conversion*, a mechanism used in quantum optics to generate non-classical states of light. The parametric amplifier for matter waves is an important tool for tasks ranging from fundamental investigations of quantum mechanics e.g. in chapters 3 and 4 to *proof-of-principle* experiments e.g. in section 2.3.

In order to understand and control the complex nature of spin-changing collisions the relevant energy scales have to be considered. There are three contributions, namely the magnetic-field dependent energy shift, collisional interactions and the trapping potential. The former is well described by the linear and the quadratic Zeeman effect since we are working at small magnetic fields ($B < 3\,\text{G}$). Due to the conservation of magnetization (2.1) the linear Zeeman effect can be neglected and only the small quadratic Zeeman effect contributes to the overall shifts in energy. It has an opposite sign for the two hyperfine manifolds of ^{87}Rb. In $F = 1$, the energy of a pair of atoms in $m_F = 0$ is smaller than the energy of one atom in $m_F = -1$ plus the energy of another atom in $m_F = +1$ (we label this energy difference by $2q$). In $F = 2$, the situation is reversed. The second contribution - the collisional interactions - can be restricted to collisions that involve atoms in $m_F = 0$ since the density of particles in all other states is very small. Three relevant collision terms remain [52]:

- The term for collisions between atoms in $m_F = 0$ without spin change, labeled U_0
- The term for two atoms in $m_F = 0$ transferred to $m_F = \pm 1$ and the reverse process, labeled U_1
- The term for collisions between one atom in $m_F = 0$ and the other in $m_F = \pm 1$, labeled U_{10}. Calculations show $U_{10} = U_0 + U_1$.

These parameters differ for the two hyperfine states. The influence of the interaction strength U is density dependent. Therefore, the effect is linked to the trapping potential V_{ext} - the last important energy scale for spin dynamics. An effective confinement for atoms in $m_F = \pm 1$ can be given as

$$V_{\text{eff}}(\mathbf{r}) = V_{\text{ext}}(\mathbf{r}) + (U_0 + U_1)\, n_0(\mathbf{r}) - \mu\,, \tag{2.2}$$

where $\mathbf{r}$ is the spatial coordinate, n_0 is the density of the $m_F = 0$ condensate and the chemical potential μ is subtracted to set the energy of an atom in $m_F = 0$ to zero. The single particle Hamiltonian is then

$$H_{\text{eff}}(\mathbf{r}) = -\frac{\hbar^2}{2m}\Delta + V_{\text{eff}}(\mathbf{r})\,. \tag{2.3}$$

For simplicity a single eigenmode denoted by ϕ with a corresponding eigenenergy E is considered. By introducing the bosonic creation (annihilation) operator $a^\dagger_{\pm 1}$ ($a_{\pm 1}$) and assuming that the mode ϕ is equal for atoms in $m_F = +1$ and $m_F = -1$, we obtain the Hamiltonian

$$H = \underbrace{(E+q)\,(a^\dagger_{+1}a_{+1} + a^\dagger_{-1}a_{-1})}_{\text{eigenmode and Zeeman energy}} + \underbrace{i\,(\Omega^* a_{+1}a_{-1} - \Omega\, a^\dagger_{+1}a^\dagger_{-1})}_{\text{spin dynamics}}\,. \tag{2.4}$$

$\Omega = 2CN_0U_1$ is the spin dynamics rate and C depends on the overlap integral of the two particles in the mode ϕ with the $m_F = 0$ condensate of N_0 atoms. Using the Heisenberg equation $i\frac{d}{dt}a = [a, H]$ with $\hbar = 1$ we can calculate the transfer of atoms from the $m_F = 0$ condensate to $m_F = \pm 1$. The solution is a set of coupled equations which can be solved by a Bogoliubov transformation. The new operators $b_\pm(t) = e^{\mp it\lambda}b(0)$ evolve with eigenvalues

$$\lambda_\pm = \pm\sqrt{(E+q)^2 - |\Omega|^2}\,. \tag{2.5}$$

These Bogoliubov modes become unstable if the eigenvalues λ are imaginary. The modes are most unstable if the eigenenergy E and the Zeeman energy cancel each other. Since there is an infinite number of eigenmodes with corresponding eigenenergies E_n, there is a multiresonant spin dynamics behavior [53]. The instability rate $\text{Im}(\lambda)$ describes half circles centered at E_n with radii $|\Omega_n|$. Consequently, several competing modes can be amplified simultaneously which demands careful consideration to operate in a single-mode regime. This is important for the contrast in atom interferometry (see section 2.3) and if a homodyne detection is used (section 3.3 and 4.3). Therefore, it is beneficial to perform spin dynamics in the $F = 1$ manifold, since Ω depends on the interaction strength U_1 which is significantly smaller compared to $F = 2$. Thus, the spin dynamics resonances are much better separated and the system can be operated in a single-mode regime.

The Bogoliubov modes can be transformed back to the initial creation and annihilation operators allowing for the calculation of the mean particle number, its variance and other observables. The most important situation occurs on resonance $E = -q$, which is accessed experimentally by tuning the parameter q via the magnetic field or a microwave

dressing field [52,54,55]. The Hamiltonian (2.4) becomes equal to the two-mode squeezing operator known from optics. If it acts on the vacuum state, we recover the two-mode squeezed vacuum state. Represented in the basis of Fock states $|n_1\rangle \times |n_2\rangle = |n_1, n_2\rangle$, where n_1 and n_2 denote the number of atoms in the two levels $m_F = \pm 1$, we get

$$|\xi\rangle = \sum_{n=0}^{\infty} \frac{(-i \tanh \xi)^n}{\cosh \xi} |n, n\rangle \ , \tag{2.6}$$

where $\xi = \Omega t$ is the squeezing parameter. This state has important properties like vanishing population imbalance between the two modes, a squeezed phase sum and squeezed and anti-squeezed quadrature variances. These correlations are illustrated in the following chapters.

2.2 Spontaneous symmetry breaking in spinor Bose-Einstein condensates

Spontaneous symmetry breaking constitutes an important mechanism in many fields of physics [56]. For instance, it occurs in cosmology [57], particle physics [58] and superfluid helium [59]. The dynamical evolution of a system can be determined by small fluctuations which do not reflect the underlying symmetry of the system. BECs are suitable to explore symmetry-breaking processes [60] and investigate nonequilibrium dynamics like the formation of topological defects via the Kibble-Zurek mechanism [57, 59] as well as provide a detailed insight into dynamical symmetry breaking. Experimental realizations contain vortex formation [61], spinor BECs [62,63], and BECs with dipolar interactions [64]. Furthermore, it is an important step in understanding BECs and their coherence properties [65,66].

Ref. [A1] reports on a ^{87}Rb spinor BEC in a crossed-beam optical dipole trap with two identical trap frequencies. Thus, a cylindrical symmetry is inherent to the system. A closer look at the effective potential (2.2) allows for several simplifications resulting in an analytically solvable single-particle Hamiltonian and thus, leads to a deep insight into the underlying mechanism. The harmonic confinement $V_{\text{ext}}(\mathbf{r})$ for atoms in $m_F = \pm 1$ is heavily affected by the presence of the strong $m_F = 0$ condensate (see (2.2)). The density profile of the $m_F = 0$ condensate n_0 reflects the external trapping potential and is approximately $n_0(\mathbf{r}) \approx U_0^{-1}(\mu - V_{\text{ext}}(\mathbf{r}))$. The repulsive interaction flattens the effective potential for atoms in $m_F = \pm 1$ within the Thomas-Fermi radius. Outside the radius, the confinement due to the dipole trap rises abruptly which is approximated by steep walls. Hence, the trapping potential for atoms in $m_F = \pm 1$ is a cylindrical box potential. The eigenmodes are Bessel-like functions and can be characterize by two quantum numbers for radial excitation n and for angular momentum l. The eigenenergies of these modes are degenerate for the same values of $|l|$.

If the magnetic field is tuned to a spin dynamics resonance with $|l| \neq 0$ ($E_{n,|l|} + q = 0$ in (2.5)), two eigenmodes will be populated. One rotates clockwise ($l = +|l|$) and forms a vortex and one rotates counterclockwise ($l = -|l|$) and forms an antivortex. Every

mode taken by itself is cylindrically symmetric, however, both modes are populated at the same time and lead to an interference structure which does not reflect the symmetry of the system. The orientation of the interference pattern is governed by the phases of the two modes. In the experiment, the population of modes with $n > 1$ occurs due to parametric amplification of vacuum fluctuations, demonstrated in Ref. [67]. As a result, the phases are random. The interference structure shows an arbitrary orientation in each experimental realization. Thus, the magnetization patterns spontaneously break the spatial symmetry.

The spin symmetry can be broken as well. This was first observed in Ref. [68], where a spinor BEC was quenched from a polar into a ferromagnetic phase and a transverse magnetization spontaneously occurred. However, in our experiment, a longitudinal magnetization is also discovered. It arises if the symmetry axis of the two distributions of atoms in $m_F = +1$ and $m_F = -1$ are different. This strongly depends on the exact value of the magnetic field. The results show that spinor BECs are exceptionally controllable systems for a detailed analysis of symmetry breaking and, in particular, its close connection to multimode squeezing during parametric amplification.

2.3 Non-classical atom interferometry

As mentioned in chapter 1, atom interferometers rely on the wave nature of matter. However, the ultimate sensitivity of interferometers is limited by their particle nature and quantum mechanics itself. Each particle passing through an interferometer has to localize at the output in either one of the two ports. This results in the so-called shot noise limit for classical interferometers, which scales as $1/\sqrt{N_{\mathrm{tot}}}$ with the total particle number N_{tot}. This limit can be surpassed if the particles injected into the interferometer are entangled. These quantum mechanical correlations allow for an operation at the Heisenberg limit which scales as $1/N_{\mathrm{tot}}$. This scaling behavior can be reached with highly entangled states such as *NOON* [69] or twin-Fock states [70]. These states have only been created with few atoms or ions. Spin dynamics has been proposed to offer the possibility to create mixtures of twin-Fock states with large particle number.

In Ref. [A2], spin dynamics is used to generate twin-Fock states of up to 10^4 atoms and demonstrate an interferometric sensitivity of $-1.6^{+0.98}_{-1.1}$ dB below the standard quantum limit. This was the first demonstration that spin dynamics is suitable to generate large ensembles of entangled states. These ensembles are well described by the collective spin $\mathbf{J} = (J_x, J_y, J_z)^T$ containing the population imbalance $J_z = (N_{+1} - N_{-1})/2$, where $N_{\pm 1}$ denotes the population in the two modes $m_F = \pm 1$. It can be visualized on the generalized Bloch sphere, where J_z represents the z-axis and the azimuthal angle in the J_x-J_y plane represents the phase between the two modes (Fig. 2.1 a and b). The uncertainty of a state is depicted as an area on the sphere. For example, a coherent state has equally distributed uncertainties between population imbalance and relative phase and is represented by a circular disc on the sphere. For the twin-Fock state created by spin dynamics, the uncertainty in the population imbalance is zero ($\Delta J_z = 0$) due to the pair-creation process, and hence the relative phase is undefined since it is the conjugate

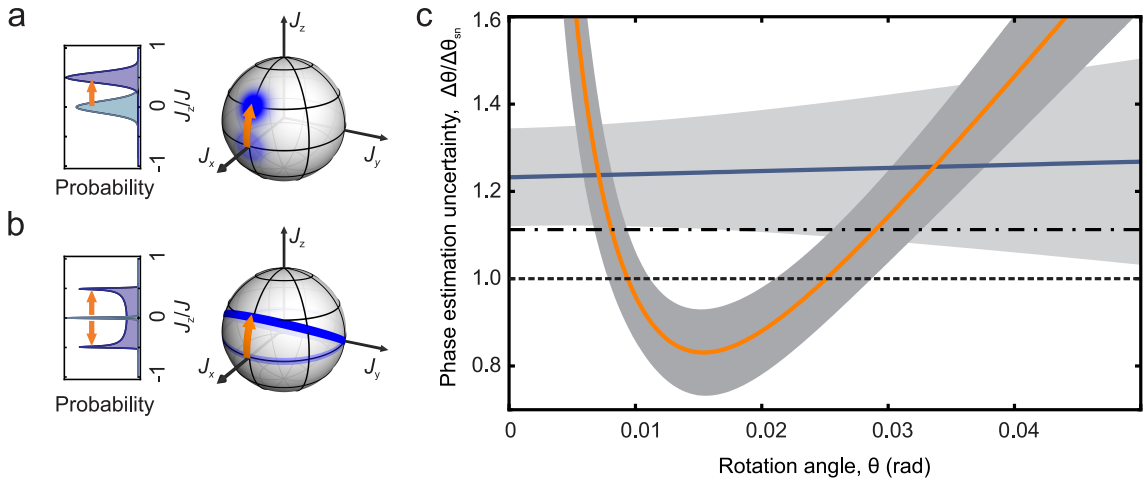

Figure 2.1: **Classical and non-classical atom interferometry.** Action of an interferometric sequence represented on the generalized Bloch sphere **a** for a coherent state and **b** for a twin-Fock state. **c** Estimated phase uncertainty determined from an error propagation for a coherent state (blue) and for the twin-Fock state (orange) compared to shot noise (dashed line) and to shot noise plus detection noise (dashed-dotted line).

observable. In the experiment, the measured variance in J_z was mainly limited by the detection noise. We obtained a suppression of $-6.9^{+0.89}_{-0.99}$ dB at $7,800 \pm 1,000$ atoms compared to shot noise.

A beam splitter for matter waves can be realized via Rabi oscillations. For a 50/50 beam splitter, the coupling field is turned off after an oscillation of $\pi/2$. A Ramsey interferometer consists of two such $\pi/2$-pulses and an evolution time between those pulses. In the case of a coherent state, the phase difference accumulated during the evolution time is imprinted on the expectation value of the population imbalance $\langle J_z \rangle$ in the output modes by the second pulse (Fig. 2.1 a). In the case of a twin-Fock state, the first $\pi/2$-pulse transforms the well-defined population imbalance into a well-defined phase at the expense of an undefined population imbalance. The phase accumulation rotates the state around the J_z-axis and the second pulse maps this well resolved phase onto the fluctuations in J_z. Hence, the variance of the population imbalance contains the interferometric signal (Fig. 2.1 b). We achieve a contrast close to the ideal one, which proves single-mode operation of the parametric amplification process. Spin dynamics time has to be chosen carefully such that a relative suppression of unwanted modes occurs and the parametric approximation still holds.

The state's interferometric sensitivity can be measured by a single rotation induced by a coupling pulse. The fluctuations were measured for different rotation angles θ and the phase estimation uncertainty $\Delta\theta/\Delta\theta_{sn}$ relative to the standard quantum limit is obtained from an error propagation (see section 2.5). The result is shown in Fig. 2.1 c. For a small rotation angle of $\theta = 0.015$ rad, the standard quantum limit (dashed line at unity) is surpassed by $-1.6^{+0.98}_{-1.1}$ dB. The enhancement is even clearer if it is compared

to a combination of shot noise and detection noise (dashed-dotted line) ($-2.5^{+0.98}_{-1.1}$ dB). The limitation of the achieved sensitivity is given by the detection noise in our experiment. The combination of large samples and quantum-enhanced sensitivity opens exciting perspectives for highly sensitive measurements with a new generation of atom interferometers.

2.4 Entanglement quantification of Dicke states

In the previous section, we have seen that entangled ensembles are useful for quantum-enhanced metrology. However, the quantification of entanglement for such large ensembles is complicated. A full state tomography is not feasible due to the exponential increase of the required number of measurements. For spin-squeezed states, entanglement is detected by a spin-squeezing parameter $\xi^2 = N(\Delta J_z)^2/(\langle J_x\rangle^2 + \langle J_y\rangle^2)$ smaller than one. The entanglement depth [23] is defined as the number of particles in the largest inseparable subset of a state and is determined from measurements of the collective spin. It has been applied in Refs. [19, 20] to demonstrate an entanglement depth of 170 and 150 atoms, respectively. This entanglement detection and quantification works for spin-squeezed states only, which represents a small subset of entangled states. In particular, it does not include Dicke states like the twin-Fock state produced by spin dynamics. The criterion is also not valid for strong spin squeezing because the denominator of ξ^2 is reduced. Hence, a generalization of the spin-squeezing parameter is required.

In Ref. [A3], such a generalized squeezing parameter [71, 72] is used. It allows for the detection of entanglement based on measurements of expectation values and their variances of the collective spin (see section 2.3). In addition, the entanglement depth of an experimentally created Dicke-like state is determined. The extension to a generalized squeezing parameter ξ^2_{gen} is based on the introduction of an effective spin length $J^2_{\text{eff}} = \langle J_x^2 + J_y^2\rangle$, which is equal to the spin length in the limit of vanishing $\langle J_z^2\rangle$. The parameter reads

$$\xi^2_{\text{gen}} = (N-1)\frac{(\Delta J_z)^2}{\langle J_{\text{eff}}\rangle - J_{\max}}, \tag{2.7}$$

where N is the number of particles and $J_{\max} = N/2$. Dicke-like atomic states can be created with various methods such as in Refs. [73, 74]. In this work, spin dynamics in a ^{87}Rb spinor BEC of 2×10^4 particles in a crossed-beam optical dipole trap is utilized to generate a Dicke-like state. In contrast to Refs. [A1, A2], spin dynamics is performed in the $F = 1$ manifold. Here, hyperfine-changing collisions are avoided and spin dynamics resonances are clearly distinct, which allows for single-mode operation of the parametric amplifier (careful considerations of the spin dynamics time as in Ref. [A2] are unnecessary). In each experimental cycle up to 8,000 particles in the $m_F = \pm 1$ state are produced via spin-changing collisions. The fluctuations ΔJ_z of the collective spin can be directly measured by counting the number of atoms in the two Zeeman levels. The fluctuations vanish, as expected for spin dynamics. For a measurement of the effective spin length J_{eff} the state is rotated by a $\pi/2$-pulse (similar to Ref. [A2]). An almost ideal effective spin length of $J_{\max} = N/2$ is observed. The combined measurements of

ΔJ_z and J_{eff} prove that the created state is in close vicinity of an ideal symmetric Dicke state. At a total of $N = 8,000$ particles, we reach $\xi^2_{\text{gen}} = -11.4(5)\,\text{dB}$. We can also infer the entanglement depth k, using a new generalized method. For every fixed value of k, a minimal achievable value for $(\Delta J_z)^2$ as a function of J^2_{eff} can be determined. A comparison with the measured values allows for an extraction of k. We find an entanglement depth of $k = 68$ atoms. The results are mainly limited by the detection noise and not by the properties of the created state itself.

2.5 Verifying metrological usefulness of Dicke states

Dicke states constitute a particular relevant class of highly entangled states. They have optimal metrological properties [75–77] and can be used to reach Heisenberg-limited sensitivity [70] as discussed in section 2.3. Symmetric Dicke states have been created with photons [75, 78, 79] as well as with cold atoms [80, A2, A3] and their metrological properties have been experimentally tested [75, A2]. However, this verification demands a large number of measurements. In Ref. [A2], a long series of measurements of the total spin of the ensemble was needed for different rotation angles θ to estimate the precision and find the optimal angle θ_{opt}, where the uncertainty $(\Delta\theta)^2$ is minimized. If an observable M is measured in an interferometric sequence (J_z^2 in Ref. [A2]), the parameter estimation uncertainty is obtained from an error propagation $(\Delta\theta)^2 = (\Delta M)^2/|\partial_\theta \langle M\rangle|^2$. The sensitivity is maximized by reducing the fluctuations in the observable M and by a steep slope $\partial_\theta \langle M\rangle$. However, for Dicke states in the presence of technical noise, the optimal sensitivity is not at $\theta = 0$ as one might expect from the noiseless error propagation. A simple procedure to find the optimal angle and to determine the best sensitivity achievable without executing the full interferometric procedure is beneficial.

In Ref. [A4], we show that the optimal angle θ_{opt} for symmetric Dicke states in the presence of technical noise can be obtained from a closed formula without carrying out the metrology itself. We also derive a closed formula for the maximal parameter estimation uncertainty $\Delta\theta$ based on the measurement of only a few expectation values. This method permits us to verify the metrological usefulness of Dicke states. Furthermore, we apply our method to the data from Ref. [A3] and show that we can detect metrological usefulness by measuring only the second moments of the collective angular momentum components. Thus, our method simplifies the experimental determination of metrological sensitivity.

3 Einstein-Podolsky-Rosen correlations with massive particles

In 1935, EPR devised a thought experiment [11], which demonstrated that quantum mechanics must be incomplete under reasonable assumptions. EPR tried to combine quantum mechanics with so-called elements of reality. But what started as a proof of the incompleteness of quantum mechanics finally challenged their assumptions - today known as locality and realism. EPR showed that quantum mechanics as a complete theory is inconsistent with local realism. The contradiction reveals strong quantum mechanical correlations, incompatible with a local realistic theory. This inconsistency demands experimental confirmation to prove that these EPR correlations are indeed physically accessible and that quantum mechanics is valid. In this chapter, we will review the original EPR thought experiment in section 3.1 and present a criterion for EPR correlations that can be verified in experiments. Afterwards, we give an overview about experiments demonstrating EPR correlations in section 3.2. Finally, we apply the criterion for EPR correlations in section 3.3 to many-particle states created by spin dynamics in a BEC. Hereby, we report the first creation of EPR correlations with massive particles.

3.1 The Einstein-Podolsky-Rosen thought experiment

In their famous publication [11], EPR posed two questions in order to benchmark the success of a physical theory: (i) *"is the theory correct?"* and (ii) *"is the description of the theory complete?"*. EPR never questioned the former, but had severe concerns about the latter regarding quantum mechanics. Therefore, EPR introduced a completeness condition: *"every element of the physical reality must have a counterpart in the physical theory"*. If a physical quantity can be predicted with certainty without disturbing the system, an associated element of reality must exist, that predetermines the outcome whether or not the corresponding measurement is carried out. In quantum mechanics, a system is supposed to be *completely* described by its wave function Ψ obeying Schrödinger's equation. For example, if the system is in an eigenstate of an operator Q, the state after the measurement is $\Psi' = Q\Psi = q\Psi$, where q denotes the corresponding eigenvalue, and thus, an element of reality must exist for the quantity Q. On the other hand, if the state Ψ is not an eigenstate of Q, a measurement is needed to determine its quantity and this will alter the state. More generally, if two operators Q and P do not commute $[Q, P] \neq 0$, the precise knowledge of one quantity precludes the knowledge of the other. Therefore, the two corresponding quantities can not have simultaneous

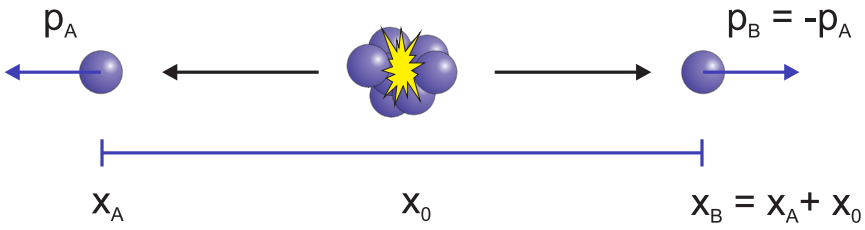

Figure 3.1: **Einstein-Podolsky-Rosen scenario.** Two particles A and B are emitted from a common source and spatially separated by x_0. Their positions x_A and x_B are perfectly correlated, whereas their momenta p_A and p_B are perfectly anti-correlated.

reality. However, A. Einstein was convinced that every measurement result can in principle be predicted with certainty, and thus, the description by the wave function can not be considered complete. Therefore, EPR constructed the following scenario intended to show the incompleteness of quantum mechanics. It presents the first demonstration of the problems that arise from the assumption of local realism in quantum mechanics.

In the EPR scenario, we consider a source emitting pairs of particles. The two particles move in opposite directions into regions A and B, respectively, which are spatially separated by x_0. The particles have perfectly correlated positions $x_\mathrm{A} = x_\mathrm{B} + x_0$ and anti-correlated momenta $p_\mathrm{A} = -p_\mathrm{B}$ (Fig. 3.1). The system is described by the two-particle wave function

$$\Psi(x_\mathrm{A}, x_\mathrm{B}) = \int_{-\infty}^{\infty} e^{(i/\hbar)\,(x_\mathrm{A} - x_\mathrm{B} + x_0)\,p}\, dp\,. \tag{3.1}$$

An observer in region A is free to choose a measurement of either the momentum P of his particle, returning some value p or the position Q, returning some value x. In order to see the consequences of a momentum measurement on particle A for the two-particle state, we rewrite the two-particle wave function in the eigenbasis of momentum states for A, $u_p(x_\mathrm{A}) = e^{(i/\hbar) p\, x_\mathrm{A}}$. The two-particle state reads

$$\Psi(x_\mathrm{A}, x_\mathrm{B}) = \int_{-\infty}^{\infty} \psi_p(x_\mathrm{B})\, u_p(x_\mathrm{A})\, dp\,, \tag{3.2}$$

where $\psi_p(x_\mathrm{B}) = e^{-(i/\hbar)\,(x_\mathrm{B} - x_0)\,p}$ is an eigenfunction of the momentum operator of particle B with an eigenvalue $-p$. Thus, by a measurement of the momentum of particle A, the momentum of particle B can be predicted with certainty. Since the particles are spatially separated, the measurement should not disturb system B according to EPR. Therefore, they conclude that an element of reality for the momentum must exist.

On the other hand, if observer A chooses to measure the position Q, he obtains a value x. Therefore, the two-particle state is written in the eigenbasis of position operator $v_x(x_\mathrm{A}) = \delta(x_\mathrm{A} - x)$. We find

$$\Psi(x_\mathrm{A}, x_\mathrm{B}) = \int_{-\infty}^{\infty} \varphi_x(x_\mathrm{B})\, v_x(x_\mathrm{A})\, dx\,, \tag{3.3}$$

where $\varphi_x(x_\mathrm{B}) = (\hbar/2\pi)\,\delta(x - x_\mathrm{B} + x_0)$ is an eigenfunction of the position operator Q of particle B with eigenvalue $x + x_0$. Accordingly, if observer A measures the position of the first particle, he can predict the position of the second particle with certainty and therefore an element of reality for the position must exist.

EPR assumed that the concept of local realism holds and consequently, the second particle can not be disturbed by any measurement performed on the first system. Therefore, the second system must be completely described by the wave functions ψ_p and φ_x simultaneously, because they belong to the same reality. But the two wave functions are clearly different and, in particular, they demand simultaneously that two elements of reality exist, which belong to two noncummuting quantities ($[Q, P] \neq 0$). However, as mentioned in the beginning, these quantities can not have simultaneous reality due to the Heisenberg uncertainty relation. Thus, an inconsistency appears and one has either to conclude that quantum mechanics is incomplete (which EPR preferred) or to abandon local realism.

The correlations implied by EPR do not allow to write equation (3.1) as a product of two individual states, meaning the state is nonseparable. Consequently, a state reduction induced by a measurement of a quantity of particle A leads also to a state reduction for particle B and vice versa. It does not depend on the spatial separation x_0, but on the observable measured at A or B, respectively. This seemingly remote-controlled behavior was termed *steering* by E. Schrödinger [10].

The perfect correlations assumed by EPR are permitted from a quantum-mechanical point of view, but they are experimentally not accessible. Hence, an extension to the concept of local realism is needed that accounts for less than perfect correlations. This problem was already considered in 1936 by W. Furry [81]. In 1989, M. Reid [26] proposed an experimentally useful criterion. It accounts for the imperfections in preparation and detection in real experiments by introducing *stochastic* elements of reality which can be predicted with some specified uncertainty. The EPR scenario remains the same but instead of the precisely defined values, a remote measurement at A allows to predict a probability distribution for the outcome of the corresponding measurement at B. These probability distributions can be characterized by their inferred variances $\Delta^2 x_\mathrm{B}^\mathrm{inf}$ and $\Delta^2 p_\mathrm{B}^\mathrm{inf}$, respectively. This gives rise to an inferred Heisenberg uncertainty relation, where a violation implies an EPR paradox [26]. The EPR criterion by M. Reid is

$$\Delta^2 x_\mathrm{B}^\mathrm{inf} \times \Delta^2 p_\mathrm{B}^\mathrm{inf} < 1/4\,. \tag{3.4}$$

This inequality is much stronger than simple inseparability. The threshold of 1/4 can be visualized as follows. We consider two identical coherent states. Each fluctuates with shot noise which is normalized to 1/2. If we infer from a measurement of one state the corresponding value of the other, the result will fluctuate with two times shot noise. In order to infer values better than shot noise of the single state, the noise in each state must be reduced by at least 3 dB, thus, the threshold for the violation of an inferred Heisenberg relation is 1/4.

The inequality provides the possibility to test the inconsistency of quantum mechanics and local realism. It has been applied to various experimental realizations in the recent years as we will see in section 3.2 and in Ref. [A5] which we will discuss in section 3.3.

The conclusion in the original EPR publication [11] is that quantum mechanics must be completed by the elements of reality or more general by *local* hidden variables. This inspired the work of J. Bell [25], who derived inequalities (known as Bell inequalities) that show a measurable difference between the prediction of quantum mechanics and local hidden variable theories (LHVTs) for a certain class of states (called Bell states). A violation of a Bell inequality proves that LHVTs are not compatible with the experimental measurements. Although, such tests of quantum mechanics versus LHVTs are important and insightful, a demonstration of the EPR paradox presents an independent scientific objective. There are alternative theories to quantum mechanics that are not disproved by violations of a Bell inequalities [28], for instance, spontaneous decoherence [82, 83], gravitational nonlinearity [84, 85] and absorber theories [86]. Therefore, EPR experiments are an essential complement to Bell tests and further steps like spatial separation for massive EPR states are of fundamental importance as a prove of quantum mechanics.

3.2 Experimental realizations

The continuous-variable EPR proposal was not experimentally realizable at the time, thus, the early work was based on an adaption of the EPR paradox to discrete variables [28]. The following description is restricted to the continuous-variable realizations. As proposed by M. Reid [26], the EPR paradox can be demonstrated by measuring the amplitude and phase quadratures of squeezed light. The first demonstration of EPR correlations with continuous variables was realized with entangled photons by Ou et. al. [27]. They employed type II down-conversion in a subthreshold optical parametric oscillator (OPO). The signal and idler modes were then spatially separated and their quadratures were analyzed by two balanced homodyne detectors. The left-hand side of the inequality (3.4) can be used to quantify the degree of EPR paradox. Ou et. al. achieved a degree of EPR paradox of 0.175 ± 0.0025. Further demonstrations based on type II down-conversion can be found in Refs. [87–90]. EPR correlations were also achieved in spontaneous parametric down-conversion of type I in Ref. [91] and in a non-degenerate OPO [92]. Also two individual optical parametric amplifiers combined at a beam splitter can be utilized as demonstrated in Refs. [93–95]. Furthermore, a Kerr nonlinearity was implemented in Ref. [96] to generate two amplitude-squeezed fields which interfered and generated an EPR-like state. An interesting difference between these publications is the way how the states are analyzed. In Refs. [27, 87, 88, 93–97] a homodyne detection was used to obtain the quadratures. In Refs. [89–91] electron-multiplying charge-coupled devices were utilized to record the position and momentum by measuring in the near field plane and the far field plane of the nonlinear crystal, respectively.

Aside from Ref. [A5], EPR correlations have only been created with photons, while the demonstration of such strongly correlated states with massive particles was outstanding. A continuous-variable entanglement between massive particles was achieved in the group of E. Polzik [31]. They entangled 10^{12} Cs atoms in vapor cells at room temperature

by a detuned light pulse similar to a *quantum non-demolition* (QND) measurement of the collective spin of the samples. It allowed for a clear violation of an inseparability criterion [29,30] proving the entanglement of the system, but did not meet the stronger EPR criterion.

A further step was reported by the group of M. Oberthaler [32], where a homodyne technique for matter waves was demonstrated for the first time. This constitutes an atomic equivalent to a method successfully employed in optics. The entangled particles were created by spin dynamics in a BEC leading to continuous-variable entangled states. Subsequently, the states were coupled to a local oscillator by a radio frequency pulse to perform the homodyning. The inseparability criterion was fulfilled, however, the inequality (3.4) necessary for a demonstration of EPR paradox was not met.

3.3 First demonstration of Einstein-Podolsky-Rosen correlations with massive particles

In Ref. [A5], we fulfill M. Reid's criterion (3.4) with states of massive particles created by spin dynamics. The basic idea is to generate a two-mode squeezed vacuum $|\xi\rangle$ (2.6), where ξ is the squeezing parameter. It exhibits continuous-variable entanglement. These variables are represented by amplitude $x_{\mathrm{A/B}}$ and phase $p_{\mathrm{A/B}}$ quadratures, satisfying the commutation relation $[x_{\mathrm{A/B}}, p_{\mathrm{A/B}}] = i$. The two modes correspond to systems A and B. Position and momentum operators in the genuine EPR scenario are replaced by the quadratures $x_{\mathrm{A/B}} = (a^\dagger_{\mathrm{A/B}} + a_{\mathrm{A/B}})/\sqrt{2}$ and $p_{\mathrm{A/B}} = i\,(a^\dagger_{\mathrm{A/B}} - a_{\mathrm{A/B}})/\sqrt{2}$ respectively. A homodyne detection allows for an accurate experimental access to these quadratures both in optics and in atom optics [32]. The correlations are revealed in four two-mode variances $V_x^\pm = \mathrm{Var}(x_\mathrm{A} \pm x_\mathrm{B}) = e^{\pm 2\xi}$ and $V_p^\pm = \mathrm{Var}(p_\mathrm{A} \pm p_\mathrm{B}) = e^{\mp 2\xi}$, which fulfill M. Reid's criterion (3.4) $V_x^+ \times V_p^- < 1/4$ for sufficiently large squeezing. In the limit of infinite squeezing $\xi \to \infty$ we recover the perfect correlations implied by EPR.

In the experiment, we create a BEC of 2×10^4 ^{87}Rb atoms, initially prepared in ($F = 1$, $m_F = 0$). Subsequently, we initiate spin dynamics and populate the states $m_F = \pm 1$ within $t = 26\,\mathrm{ms}$ and a spin dynamics rate of $\Omega = 2\pi \times 5.1\,\mathrm{Hz}$. This ideally yields the two-mode squeezed state (2.6), characterized by $\xi = \Omega t$. We use an unbalanced homodyne detection realized by a radio frequency coupling of 15 % of the remaining condensate to the ± 1 modes. The condensate acts as a local oscillator. Its phase θ can be tuned via an adjustable holding time, hence it allows to measure the x and p quadratures (Fig. 3.2 a) as well as any linear combination

$$\mathrm{X}_{\mathrm{A/B}}(\theta) = x_{\mathrm{A/B}} \cos(\theta - \frac{\pi}{4}) + p_{\mathrm{A/B}} \sin(\theta - \frac{\pi}{4})\,. \tag{3.5}$$

In Fig. 3.2 b, we show the variances $V^+_{\mathrm{X}(\theta)}$ and $V^-_{\mathrm{X}(\theta)}$ as a function of the local oscillator phase θ of a total of more than 2800 measurements. At $\theta = 3/4\,\pi$ and $\theta = 5/4\,\pi$, the x and p quadratures are measured and the corresponding variances show a maximum/minimum. Based on these measurements, we can calculate the EPR violation according to equation (3.4) as shown in Fig. 3.2 c. The inseparability criterion is shown

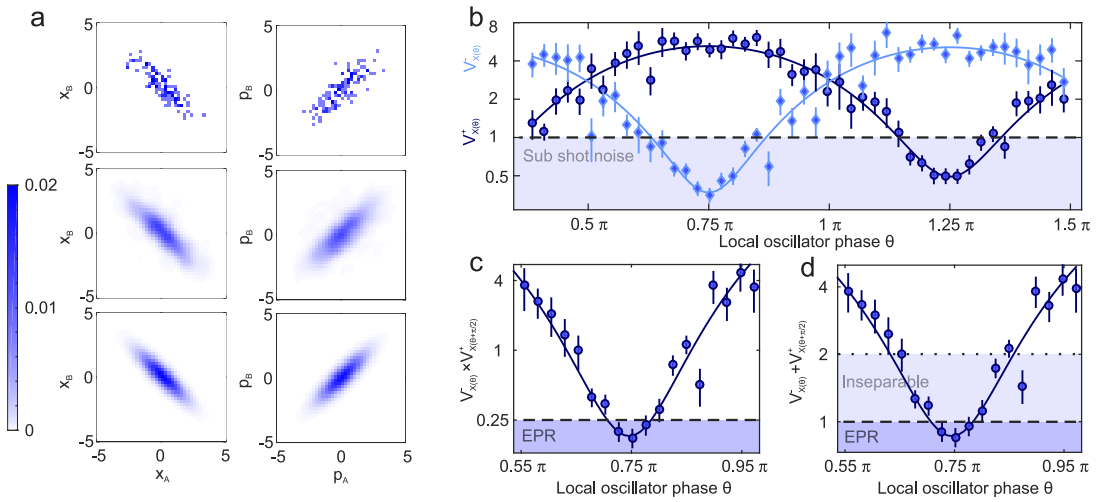

Figure 3.2: **EPR correlations.** **a** Measured quadrature distributions (first row). Distributions according to the reconstructed state (second row). Ideal distributions of the quadratures of a two-mode squeezed state with the reconstructed squeezing parameter $\xi_{\text{fit}} = 0.63$ (third row). **b** Two-mode variances $V^{+}_{\text{X}(\theta)}$ and $V^{-}_{\text{X}(\theta)}$ as a function of the local oscillator phase θ. **c** EPR parameter $V^{-}_{\text{X}(\theta)} \times V^{+}_{\text{X}(\theta+\frac{\pi}{2})}$ as a function of the local oscillator phase θ. Data points below the dashed line fulfill the EPR criterion. **d** The weaker inseparability parameter $V^{-}_{\text{X}(\theta)} + V^{+}_{\text{X}(\theta+\frac{\pi}{2})}$ as a function of the local oscillator phase θ. The dotted line indicates inseparability. The dashed line is a sufficient condition for the EPR criterion.

in Fig. 3.2 d. Following M. Reid's criterion, we find a value of $V_x^+ \times V_p^- = 0.18$ with 2.4 standard deviations below the threshold of 1/4 which clearly shows the correlations necessary to demonstrate the EPR paradox. Our data also fulfills the inseparability criterion [29, 30] $V_x^+ + V_p^- < 2$ with a value of 0.852 which is 15 standard deviations below the classical threshold of 2. The results are well explained by radio frequency noise during the homodyning pulse of 0.4 % and phase noise in the local oscillator of $0.044\,\pi$.

The demonstrated strong form of entanglement is vital for a realization of the continuous-variable EPR paradox with massive particles. Prospectively, spatial separation of the two modes can be achieved with an inhomogeneous magnetic field due to their opposite magnetic moment. Additionally, a precise atom number detection could be implemented to violate a Clauser-Horne-Shimony-Holt-type inequality. Such a measurement would constitute a test of local realism with continuous-variable entangled states.

4 Quantum Zeno suppression of spin dynamics and interaction-free measurements

This chapter gives an introduction into the counterintuitive consequences which can arise from measurements in quantum mechanics. A frequent observation of a quantum-mechanical system may hinder or even freeze the expected evolution. This is called *Zeno's paradox in quantum theory*, which will be discussed in section 4.1. The collapse of the wave function also allows for the detection of an object without interacting with it. These so-called interaction-free measurements (IFMs) can be combined with the quantum Zeno effect resulting in a high-efficiency IFM, which is studied in section 4.2. Aside from Ref. [A5], these IFMs have only been realized with single photons and neutrons. In section 4.3, a multi-particle IFM with atoms is presented.

4.1 The quantum Zeno effect

In 1977, B. Misra and E. Sudarshan [33] found a seemingly paradoxical behavior in the temporal evolution of quantum-mechanical systems under repeated observation. They theoretically investigated an unstable quantum system. The evolution under frequent observation can be described as a fast sequence of infinitesimal time steps of coherent time evolution followed by projective measurements. These measurements yield a "yes-or-no" result whether the system is in a decayed state or remained in its initial state. This would provide exact knowledge of the time of decay. Surprisingly, B. Misra and E. Sudarshan found that if one tries to infer the moment of decay, the particle will never decay. Hence, the quantum mechanical state cannot evolve under frequent observation. This resembles a famous paradoxes by Zeno, who denied that a flying arrow moves, if the arrow's position is observed. The quantum version was thus named quantum Zeno effect (QZE).

The correctness of this theoretical result was questioned in the very same publication [33], since it leads to the assumption that the survival time of a radioactive particle must exhibit an increase if it is in a bubble chamber and thus under frequent observation. However, this was not experimentally verified.

The apparent discrepancy can be resolved by looking at the important time scales of the system. B. Misra and E. Sudarshan presumed an idealized measurement, that measures instantaneously. This assumption is only true if the evolution time scale is slow compared to the response time of the measurement device. On short time scales,

the probability that the system occupies a certain state changes quadratically with time. This is an important prerequisite for the quantum Zeno effect. This time scale is given by the jump time, which is on the order of $\tau_J \sim 10^{-21}$ s [98] for radioactive particles. The important criterion for determining whether the decay is hindered or not is a comparison of the jump time and the response time [99]. The latter is much longer than 10^{-21} s for a bubble chamber and, consequently, the survival time of a radioactive particle is not influenced by this observation. We conclude that the instantaneous character of the measurement is crucial for the existence of the QZE and it depends on the response time of the measurement process compared to the time scale of the quantum-mechanical evolution of the system. In general, if the measurements are non-ideal *quantum measurement theory* has to be applied. It allows to observe the QZE without the application of the projection postulate as described in Ref. [100].

While it is thus difficult to realize the QZE for radioactive decay, the quantum Zeno effect can be observed experimentally by simulating an unstable particle. This can be achieved via Rabi oscillations between two states introduced by microwave or light fields. The frequency of these oscillations can be varied by changing the intensity of the coupling field and thus, the time scale of the quadratic evolution can be easily adjusted. The projective measurement can be implemented by laser light that is resonant to one of the two levels involved in the Rabi oscillations and leads to spontaneous emission. By collecting the scattered photons, the particles' state can be observed. This was demonstrated for the first time in the group of D. Wineland [34] with $5,000$ $^9Be^+$ ions with a driven radio frequency transition between two ground-state hyperfine levels. The observation was realized by a pulsed (instead of a continuous) laser field. The QZE was also demonstrated with a single $^{172}Yb^+$ [101] and $^{171}Yb^+$ ion [102]. The first continuous QZE was observed in a slowdown of nuclear-spin conversion of the isomers of $^{13}CH_3F$ molecules [103]. Furthermore, the effect was observed in optical pumping of laser cooled $^{24}Mg^+$ ions [104] and later with neutral ^{85}Rb atoms in vapor cells at room temperature [105]. The quantum Zeno effect with BECs was studied in Ref. [35], where the first quantitative comparison between pulsed and continuous observation was performed. The authors used a ^{87}Rb condensate in a magnetic confinement and coupled two trapped states via a two-photon transition. Later, BEC experiments demonstrated Zeno suppression based on observation via a focused electron beam [106]. Instead of a freezing of the evolution, the Zeno dynamics also allows to protect a subspace [37] as predicted in Ref. [38] to realize increased coherence times. Here, a spinor BEC was created and a resonant radio frequency induced Rabi oscillations between multiple states. This evolution was subsequently tailored via the QZE.

There are numerous examples of the QZE in driven systems, however, beside Ref. [A6], the QZE in spontaneously decaying systems has only been reported in Ref. [36] due to the usually short jump times. These systems are of particular importance, since they offer the possibility to reduce particle losses. In the group of M. Raizen [36], a system of cold Na atoms in an accelerated optical lattice was investigated. By varying the acceleration of the lattice, it was possible to switch between spontaneous decay of trapped atoms via tunneling to higher bands, and spatial separation of these decayed atoms from the remaining atoms which acts as a measurement. The jump time could be tailored to

a few microseconds by designing the band structure of the lattice appropriately. The system showed the first experimental evidence for a deviation from the exponential decay law [107]. The observed deviation allowed also to demonstrate the so-called anti-Zeno effect [108]. However, the setup has three disadvantages. First, it is not possible to observe continuously. Second, the time needed for the measurement is rather long compared to the tunneling time. As a consequence, the time axis must be rescaled to correct for the measurement time in order to observe the Zeno effect. Furthermore, it is a direct measurement since the potential of the undecayed atoms is altered to perform the measurement. Therefore, it is less surprising that the evolution of the system is affected compared to an indirect, negative-result measurement. We circumvent these drawbacks in a realization of the quantum Zeno effect in an unstable system presented in Ref. [A6]. It presents the first demonstration of the QZE in an unstable system with an indirect, negative-result measurement.

Aside from the fundamental interest in the QZE, it offers applications in interaction-free measurements (see next section) such as counterfactual quantum computation [45] or to suppress failure events in quantum computation [109]. More importantly, it also allows to tailor a small subsystem within a complex multilevel system and suppress decoherence [38, 110] and protect entanglement [39].

4.2 Interaction-free measurements

To recognize the presence of an object in our everyday life, we need some kind of interaction with this object. We have to touch it or force it to produce a sound. Even if we only look at it, we need light that interacts with the object in order to be able to see it. In quantum mechanics, however, an interaction-free measurement can be realized. If a measurement turns out to be a "negative-result measurement" (M. Renninger [111]) it seemingly did not disturb the system. Of course, this is an artifact originating from a certain interpretation of quantum mechanics, where we assume that only one branch of a superposition existed instead of a collapse of the wave function. This gave rise to the concept of interaction-free measurements considered by R. Dicke [112]. In 1993, A. Elitzur and L. Vaidman (EV) extended this idea in a thought experiment [41] to ascertain the presence of an object without interacting with it. This presents another manifestation of nonlocality of quantum mechanics, because the reduction of the wave packet is a global intervention.

EV illustrated their thought experiment in a dramatic way. The object, whose presence shall be detected, is an ultra-sensitive bomb that explodes if it is hit by a single photon. The question EV posed was whether it is possible to detect this object (with photons) without exploding it. Their method is based on a Mach-Zehnder interferometer with equal arm lengths. Thus, the interferometer has a bright output port, where all photons exit the interferometer, and a dark output port, where no photons arrive. This is still true if the interferometer operates with single photons, since every photon is transferred at the first beam splitter into a superposition of being in the upper arm and being in the lower arm. The two branches are then recombined at the second beam

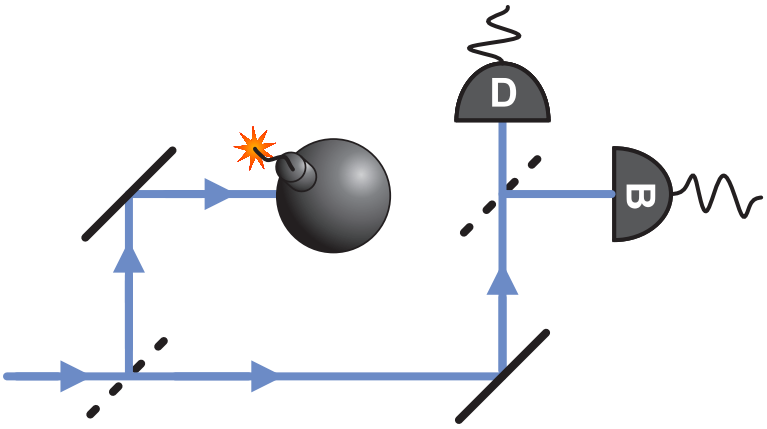

Figure 4.1: **Interaction-free measurement** as proposed by A. Elitzur and L. Vaidman [41]. A Mach-Zehnder interferometer with equal arm lengths has one bright output port, where 100 % of the photons arrive, and a dark one. An ultra-sensitive object (bomb) placed in one arm destroys the interference and photons may arrive at the dark detector, thereby witnessing the presence of the object without exploding it.

splitter and interfere. The interference leads to the result described above. EV proposed to place the ultra-sensitive object in one arm of the interferometer as illustrated in Fig. 4.1. The object is considered to be classical, thus, when the corresponding branch of the superposition reaches the position of the object the wave function will collapse and the photon will localize either in the upper arm leading to an explosion or in the lower arm. In the latter case, the photon arrives at the second beam splitter and may exit the bright output port, which gives no information about the object and the measurement must be repeated. Or it exits the dark output port and thereby witnesses the presence of the object without exploding it. The optimal achievable efficiency η_{IFM} with this setup is an interaction-free measurement of $\eta_{\mathrm{IFM}} = 50\,\%$.

The first demonstration of an interaction-free measurement was achieved in 1995 by Kwiat et. al. [42]. They employed spontaneous parametric down-conversion in a $LiIO_3$ crystal to generate pairs of photons. By using the strong time and momentum correlations of these pairs [113] a single-photon Fock state can be prepared. This photon was sent into a Michelson interferometer containing an absorbing object. The obtained efficiency η_{IFM} was close to the ideal value of 1/2. Interaction-free measurements have also been tested with classical light fields attenuated to the single-photon level [114] and neutron interferometry [115]. The first application in absorption-free imaging was demonstrated in [116].

The classicality of the object leads to the fact that an interaction with it has the same effect as a measurement. The wave function of the photon collapses instead of transferring the object into a superposition of exploded and unexploded. Hence, the object is equivalent to an observation by a third party. Thus, the presence of the object can lead to the QZE which can be of great benefit to further improve the efficiency of

the IFM. This was first suggested by Kwiat et. al. [42]. By testing the presence of the object weakly but repeatedly, the efficiency of the IFM can be increased to unity. As a possible realization, the authors proposed a single photon in a system of two cavities which are weakly coupled via a semitransparent mirror. Starting with a single photon in the left cavity and without the object, the photon will evolve coherently from the left side to the right leading to a 100 % probability to find the photon in the right cavity after a fixed time T (and a superposition in between). On the other hand, if the object is placed in the right cavity, the photon can not evolve coherently and every formation of a superposition will immediately collapse. Thus, the photon localizes in the left cavity. By measuring if the photon is still in the left cavity after time T, the object is detected without explosion. In the limit of weak cavity coupling, the ideal efficiency of this measurement is 100 %.

An equivalent scheme was realized in Ref. [43], where the rotation of the polarization of a single photon was hindered via the QZE, witnessing the presence of the object. The achieved efficiency was $\eta_{\mathrm{IFM}} = 63\,\%$. It was limited by imperfections of the optical elements and interferometer instability, despite an active stabilization. Similar efficiencies were achieved with integrated quantum photonics [117] where a chain of Mach-Zehnder interferometers with weak coupling (an equivalent scheme also proposed in [42]) can be fabricated in an on-chip realization which could be useful in spectroscopic studies of photosensitive materials. Furthermore, the QZE in IFM can be used for all-optical switching [44] or to perform counterfactual quantum computation [45]. In the latter, a quantum computer is put into a superposition of 'running' and 'not running' and the potential outcome can be inferred even if the computer was not running. It was believed that counterfactual quantum computation can not perform better than random guesses [118]. However, in Ref. [45], it is demonstrated that an implementation of the QZE allows to surpass this limit. An interesting future application of IFM with the QZE is proposed in Ref. [46], where the sample damage in an electron microscope is eliminated. This is of special interest, since it is a limiting factor in imaging of biological or other specimens. Another interesting realization is an IFM with ultracold atoms. This has only been reported in Ref. [A6] and it opens the field of counterfactual quantum information to atom optics.

4.3 Multi-particle interaction-free measurements with atoms by quantum Zeno suppression

We already discussed the observation of the quantum Zeno effect in ultracold atoms and unstable systems in section 4.1 and the criticism concerning the simulated instability and direct measurements. These drawbacks are avoided in a scheme proposed by A. Luis and J. Peřina [119], where the decay products of an unstable system are measured (indirect measurement) and a negative-result measurement is performed. This constitute the most interesting scenario, because seemingly nothing happens in the case of an indirect, negative-result measurement, and thus, one would expect the system to be completely

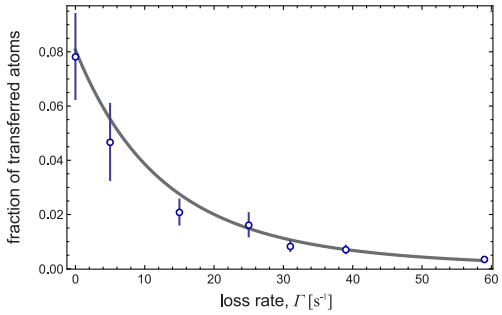

Figure 4.2: **Quantum Zeno effect in spin-changing collisions.** The fraction of transferred atoms to $(1, +1)$ as a function of the effective loss rate during 200 ms spin dynamics time. The gray line is a theory curve without free parameters.

undisturbed [120]. A. Luis and J. Peřina suggest to use parametric down-conversion in a nonlinear crystal. Photons of a pump field can spontaneously decay into pairs of photons with half the energy. The authors propose to cut the nonlinear crystal into many pieces. Generated photons in the signal beam will be detected with a photo diode after each piece. Thereby, the exact moment of decay of photons in the pump field is determined. Due to the strong correlation between signal and idler photons, a Zeno suppression for the idler photons should be obtained as well.

For a real implementation with photons, the concept seems to be impossible, because cutting a nonlinear crystal into many pieces without disturbing the evolution of the pump field is challenging. However, the analog of this scheme with ultracold atoms is feasible and it is even improved, because continuous observation is also possible. We realize such a scheme in Ref. [A6] with spin dynamics in a ^{87}Rb BEC in $F = 1$. The spontaneous decay is controlled via microwave dressing on the transition $(F = 1, m_F = -1) \rightarrow (2, -2)$. The Zeno measurement is achieved by adding a laser field resonant to $F = 2$. In combination with the dressing field, it results in a loss/observation rate that acts only on atoms in $(1, -1)$. The remaining $F = 1$ levels are unaffected due to a large detuning to the dressing field. The loss rate is controlled by changing the intensity of the laser. In the experiment, we observe a suppression of spin-changing collisions, which we measure by counting the atoms in the unperturbed state $(1, +1)$. The result is depicted in Fig. 4.2. We find a decreasing transfer of atoms with increasing loss rate Γ. The gray line is a theoretical prediction without free parameters, showing that the mechanism is well understood. This is the first demonstration of the quantum Zeno effect with a continuous, indirect, negative-result measurement on an unstable system, which can be regarded as the most stringent demonstration [100].

As described in section 4.2, the quantum Zeno suppression can be applied for a high-efficiency IFMs. In our scheme, the laser field takes the role of the object/bomb. Its presence is ascertained by measuring the number of atoms transferred to $(1, +1)$. In the limit of zero transferred atoms the object is detected without scattering a single photon, hence it allows for an IFM. However, a proof of an IFM requires a detection

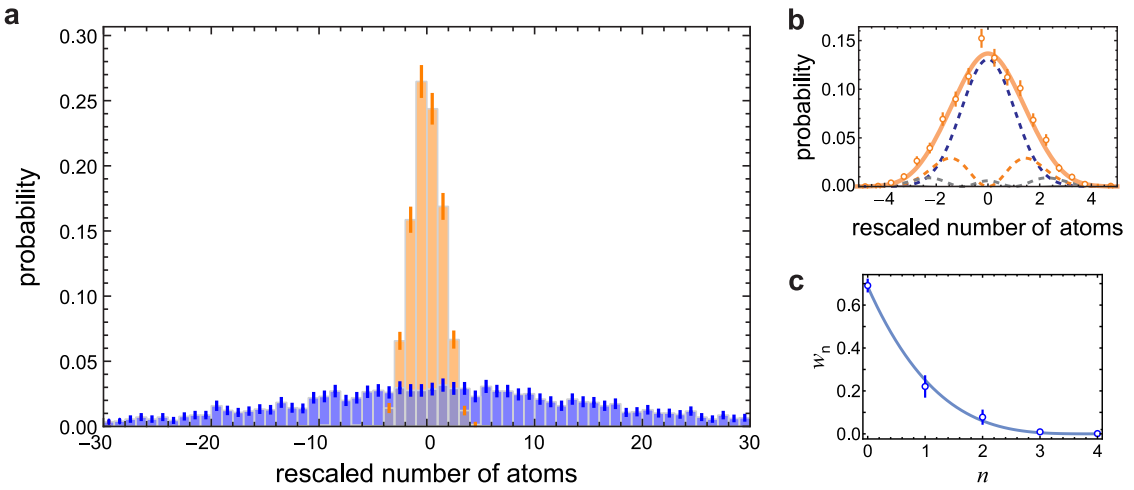

Figure 4.3: **Analysis of the interaction-free measurement.** **a** The counting statistics after unbalanced homodyning can be used to clearly distinguish between the 'with object' (orange) and 'without object' case (blue). **b** The counting statistics of the 'with object' case (orange, solid line) is reconstructed by the characteristic distributions of displaced Fock states (dashed lines). **c** Contribution of the individual Fock states. The largest contribution is the vacuum state which demonstrates the interaction-free character of our measurement.

that can distinguish between zero and one or more atoms in $(1, +1)$. This constitutes a considerable challenge due to the detection noise of 15 atoms. We overcome this limitation by implementing an unbalanced homodyne detection. Therefore, we transfer the remaining $m_F = 0$ condensate to $(2, 0)$ and subsequently couple them with a short microwave pulse to the atoms in $(1, +1)$. This resembles the action of a displacement operator [121]. The displacement transfers the vacuum state into a coherent state, which fluctuates with shot noise. Nonzero Fock states are transferred into characteristic distributions with variances that increase linearly with the number of particles. Two histograms are shown for the 'with' (orange) and 'without object' (blue) case in Fig. 4.3 a. The counting statistics for the 'with object' case shows small fluctuations, whereas the 'without object' case exhibits strong fluctuations. To reveal the interaction-free character of our measurement the 'with object' case is further analyzed.

The contributions of the different Fock states are obtained from a Maximum Likelihood analysis to reproduce the measured counting statistics (Fig. 4.3 b). The resulting contributions are depicted in Fig. 4.3 c. We find that three- and four-particle states do not contribute and one- and two-particle states sum up to a fraction of 33 %. From a background measurement, we infer that these contributions originate from residual radio frequency noise in our system. Despite this noise source, we determine a 67 % contribution of the vacuum state which clearly proves the interaction-free character of our measurement. Experimentally, objects can only be detected with a finite confidence. Therefore, we generalized the figure of merit in Ref. [41] and obtain 65 % with a 90 % confidence.

Our analysis shows that highly efficient IFMs can be realized in BECs with unstable spin configurations. Preceding experiments have demonstrated the QZE with BECs, but a proof of an IFM demands a suppression and detection on the single-particle level, which was first demonstrated in Ref. [A6]. IFMs are distinguished in two groups whether an interaction with the object can be detected or not. This scheme realizes the strong version of IFMs without requiring a single-particle source. Furthermore, it is weakly sensitive to losses due to the many-particle probe and only weakly affected by decoherence. By reducing the noise of the environment and improving the atom counting, this method permits an efficiency of 100 %.

5 Outlook

The presented results demonstrate that spin dynamics constitutes an exciting tool to generate entangled states of matter. The close analogy to optical parametric down-conversion opens the broad field of quantum optics to ultracold atoms.

Further investigations will concentrate on steering [10, 12]. The term was coined by E. Schrödinger to describe the instantaneous influence a measurement of one party in the EPR thought experiment has on the other party. The concepts of nonlocality and inseparability are symmetric between the two systems [122]. However, the concept of steering has an intrinsic asymmetry. The implied direction between the parties arose the question whether there are bipartite states that exhibit steering in only one direction [122, 123]. The states discussed in chapter 3 show steering in both directions. However, a *one-way-steering* scenario was realized with entangled modes of light from parametric down-conversion in Ref. [124]. After separating the two modes, the authors admixed a variable amount of vacuum to one of the modes. This introduces an asymmetry. The modes were analyzed via homodyne detection. At a vacuum contribution of 50 %, the one-way steering was most obvious. We could demonstrate such a correlated state with our experiment for massive particles. It demands only minor changes compared to the experiment described in section 3.3. We need to complete the experiment with an admixture of vacuum to one of the modes. This can be realized via a microwave coupling of the state (1,1) to the vacuum state in (2,2). The remaining part of the experimental sequence stays unchanged.

Another interesting perspective is the realization of a Hong-Ou-Mandel (HOM) experiment with atoms. In the original HOM experiment, two photons arrive simultaneously at a 50/50 beam splitter, each at one port. Multi-particle interference leads to a bunching effect. The two photons will exit together at one output port. The first atomic HOM experiment has been achieved quite recently [125]. The authors utilized freely propagating twin beams of metastable ^{4}He atoms coupled via Bragg scattering on an optical lattice. However, a realization with spin dynamics and atomic homodyning is feasible as well. Spin dynamics can generate a two-mode squeezed state with only two atoms on average. The $m_F = \pm 1$ modes act as the input modes of the beam splitter. A two-photon coupling between the two states realizes the splitter. Afterwards, a homodyne detection is performed. This scheme has the advantage that it allows for a generalized HOM experiment with 4, 6 and higher numbers of particles. The bunching effect should result in odd-even oscillation of the particle number in the two modes.

The two-photon coupling also allows for the generation of single-mode squeezed vacuum states. This technique is quite common in experiments with photons. If the two beams of a two-mode squeezed vacuum are combined on a 50/50 beam splitter an amplitude-squeezed and a phase-squeezed vacuum originate. An equivalent scheme

for ultracold atoms is formally identical to the HOM experiment but spin dynamics might be applied for a longer time to generate a strong population. To our knowledge, this has not been demonstrated with ultracold atoms. Such single-mode squeezed states can improve the sensitivity in atom interferometry beyond the shot noise limit, even when they are combined with a classical coherent state [126].

In summary, the methods investigated in this work have the potential to improve the precision of atom interferometers. They enable to build next-generation inertial sensors working beyond the standard quantum limit. For example, the VLBAI (very long baseline atom interferometer) is a future precision gravimeter hosted in Hanover, which will be equipped with a source of entangled states of matter.

Bibliography

[1] K. U. Schreiber, T. Klügel, J.-P. R. Wells, R. B. Hurst, and A. Gebauer. How to Detect the Chandler and the Annual Wobble of the Earth with a Large Ring Laser Gyroscope. *Phys. Rev. Lett.*, **107**, 173904 (2011).

[2] P. Fritschel and the LIGO Scientific Collaborations. LIGO: the Laser Interferometer Gravitational-Wave Observatory. *Rep. Prog. Phys.*, **72**, 076901 (2009).

[3] H. Grote and the LIGO Scientific Collaboration. The GEO 600 status. *Class. Quantum Grav.*, **27**, 084003 (2010).

[4] I. K. Kominis, T. W. Kornack, J. C. Allred, and M. V. Romalis. A subfemtotesla multichannel atomic magnetometer. *Nature*, **422**, 596 (2003).

[5] S. Merlet, Q. Bodart, N. Malossi, A. Landragin, F. P. D. Santos, O. Gitlein, and L. Timmen. Comparison between two mobile absolute gravimeters: optical versus atomic interferometers. *Metrologia*, **47**, L9 (2010).

[6] R. Wynands and S. Weyers. Atomic fountain clocks. *Metrologia*, **42**, S64 (2005).

[7] A. D. Ludlow, T. Zelevinsky, G. K. Campbell, S. Blatt, M. M. Boyd, M. H. G. de Miranda, M. J. Martin, J. W. Thomsen, S. M. Foreman, J. Ye, T. M. Fortier, J. E. Stalnaker, S. A. Diddams, Y. Le Coq, Z. W. Barber, N. Poli, N. D. Lemke, K. M. Beck, and C. W. Oates. Sr Lattice Clock at 1×10^{-16} Fractional Uncertainty by Remote Optical Evaluation with a Ca Clock. *Science*, **319**, 1805 (2008).

[8] C. W. Chou, D. B. Hume, J. C. J. Koelemeij, D. J. Wineland, and T. Rosenband. Frequency Comparison of Two High-Accuracy Al^+ Optical Clocks. *Phys. Rev. Lett.*, **104**, 070802 (2010).

[9] S. Blatt, A. D. Ludlow, G. K. Campbell, J. W. Thomsen, T. Zelevinsky, M. M. Boyd, J. Ye, X. Baillard, M. Fouché, R. Le Targat, A. Brusch, P. Lemonde, M. Takamoto, F.-L. Hong, H. Katori, and V. V. Flambaum. New Limits on Coupling of Fundamental Constants to Gravity Using ^{87}Sr Optical Lattice Clocks. *Phys. Rev. Lett.*, **100**, 140801 (2008).

[10] E. Schrödinger. Discussion of Probability Relations between Separated Systems. *Math. Proc. Cambridge Philos. Soc.*, **31**, 555 (1935).

[11] A. Einstein, B. Podolsky, and N. Rosen. Can Quantum-Mechanical Description of Physical Reality Be Considered Complete? *Phys. Rev.*, **47**, 777 (1935).

[12] E. Schrödinger. Probability relations between separated systems. *Math. Proc. Cambridge*, **32**, 446 (1936).

[13] K. Hammerer, A. S. Sørensen, and E. S. Polzik. Quantum interface between light and atomic ensembles. *Rev. Mod. Phys.*, **82**, 1041 (2010).

[14] J. Appel, P. J. Windpassinger, D. Oblak, U. B. Hoff, N. Kjærgaard, and E. S. Polzik. Mesoscopic atomic entanglement for precision measurements beyond the standard quantum limit. *Proc. Natl. Acad. Sci. U.S.A.*, **106**, 10960 (2009).

[15] Z. Chen, J. G. Bohnet, S. R. Sankar, J. Dai, and J. K. Thompson. Conditional Spin Squeezing of a Large Ensemble via the Vacuum Rabi Splitting. *Phys. Rev. Lett.*, **106**, 133601 (2011).

[16] R. McConnell, H. Zhang, J. Hu, S. Ćuk, and V. Vuletić. Entanglement with negative Wigner function of almost 3,000 atoms heralded by one photon. *Nature*, **519**, 439 (2015).

[17] M. H. Schleier-Smith, I. D. Leroux, and V. Vuletić. States of an Ensemble of Two-Level Atoms with Reduced Quantum Uncertainty. *Phys. Rev. Lett.*, **104**, 073604 (2010).

[18] J. Estève, C. Gross, A. Weller, S. Giovanazzi, and M. K. Oberthaler. Squeezing and entanglement in a Bose-Einstein condensate. *Nature*, **455**, 1216 (2008).

[19] T. Berrada, S. van Frank, R. Bücker, T. Schumm, J.-F. Schaff, and J. Schmiedmayer. Integrated Mach-Zehnder interferometer for Bose-Einstein condensates. *Nat. Commun.*, **4**, (2013).

[20] C. Gross, T. Zibold, E. Nicklas, J. Estève, and M. K. Oberthaler. Nonlinear atom interferometer surpasses classical precision limit. *Nature*, **464**, 1165 (2010).

[21] M. F. Riedel, P. Böhi, Y. Li, T. W. Hänsch, A. Sinatra, and P. Treutlein. Atom-chip-based generation of entanglement for quantum metrology. *Nature*, **464**, 1170 (2010).

[22] M. Kitagawa and M. Ueda. Squeezed spin states. *Phys. Rev. A*, **47**, 5138 (1993).

[23] A. S. Sørensen and K. Mølmer. Entanglement and Extreme Spin Squeezing. *Phys. Rev. Lett.*, **86**, 4431 (2001).

[24] D. Bohm. A Suggested Interpretation of the Quantum Theory in Terms of "Hidden" Variables. I. *Phys. Rev.*, **85**, 166 (1952).

[25] J. S. Bell. On the Einstein-Podolsky-Rosen paradox. *Physics*, **1**, 195 (1964).

[26] M. D. Reid. Demonstration of the Einstein-Podolsky-Rosen paradox using nondegenerate parametric amplification. *Phys. Rev. A*, **40**, 913 (1989).

[27] Z. Y. Ou, S. F. Pereira, H. J. Kimble, and K. C. Peng. Realization of the Einstein-Podolsky-Rosen paradox for continuous variables. *Phys. Rev. Lett.*, **68**, 3663 (1992).

[28] M. D. Reid, P. D. Drummond, W. P. Bowen, E. G. Cavalcanti, P. K. Lam, H. A. Bachor, U. L. Andersen, and G. Leuchs. *Colloquium* : The Einstein-Podolsky-Rosen paradox: From concepts to applications. *Rev. Mod. Phys.*, **81**, 1727 (2009).

[29] L.-M. Duan, G. Giedke, J. I. Cirac, and P. Zoller. Inseparability Criterion for Continuous Variable Systems. *Phys. Rev. Lett.*, **84**, 2722 (2000).

[30] R. Simon. Peres-Horodecki Separability Criterion for Continuous Variable Systems. *Phys. Rev. Lett.*, **84**, 2726 (2000).

[31] B. Julsgaard, A. Kozhekin, and E. S. Polzik. Experimental long-lived entanglement of two macroscopic objects. *Nature*, **413**, 400 (2001).

[32] C. Gross, H. Strobel, E. Nicklas, T. Zibold, N. Bar-Gill, G. Kurizki, and M. K. Oberthaler. Atomic homodyne detection of continuous-variable entangled twin-atom states. *Nature*, **480**, 219 (2011).

[33] B. Misra and E. C. G. Sudarshan. The Zeno's paradox in quantum theory. *J. Math. Phys.*, **18**, 756 (1977).

[34] W. M. Itano, D. J. Heinzen, J. J. Bollinger, and D. J. Wineland. Quantum Zeno effect. *Phys. Rev. A*, **41**, 2295 (1990).

[35] E. W. Streed, J. Mun, M. Boyd, G. K. Campbell, P. Medley, W. Ketterle, and D. E. Pritchard. Continuous and Pulsed Quantum Zeno Effect. *Phys. Rev. Lett.*, **97**, 260402 (2006).

[36] M. C. Fischer, B. Gutiérrez-Medina, and M. G. Raizen. Observation of the Quantum Zeno and Anti-Zeno Effects in an Unstable System. *Phys. Rev. Lett.*, **87**, 040402 (2001).

[37] F. Schäfer, I. Herrera, S. Cherukattil, C. Lovecchio, F. Cataliotti, F. Caruso, and A. Smerzi. Experimental realization of quantum Zeno dynamics. *Nat. Commun.*, **5**, (2014).

[38] P. Facchi and S. Pascazio. Quantum Zeno Subspaces. *Phys. Rev. Lett.*, **89**, 080401 (2002).

[39] S. Maniscalco, F. Francica, R. L. Zaffino, N. Lo Gullo, and F. Plastina. Protecting Entanglement via the Quantum Zeno Effect. *Phys. Rev. Lett.*, **100**, 090503 (2008).

[40] A. Smerzi. Zeno Dynamics, Indistinguishability of State, and Entanglement. *Phys. Rev. Lett.*, **109**, 150410 (2012).

[41] A. Elitzur and L. Vaidman. Quantum mechanical interaction-free measurements. *Found. Phys.*, **23**, 987 (1993).

[42] P. Kwiat, H. Weinfurter, T. Herzog, A. Zeilinger, and M. A. Kasevich. Interaction-Free Measurement. *Phys. Rev. Lett.*, **74**, 4763 (1995).

[43] P. G. Kwiat, A. G. White, J. R. Mitchell, O. Nairz, G. Weihs, H. Weinfurter, and A. Zeilinger. High-Efficiency Quantum Interrogation Measurements via the Quantum Zeno Effect. *Phys. Rev. Lett.*, **83**, 4725 (1999).

[44] K. T. McCusker, Y.-P. Huang, A. S. Kowligy, and P. Kumar. Experimental Demonstration of Interaction-Free All-optical Switching via the Quantum Zeno Effect. *Phys. Rev. Lett.*, **110**, 240403 (2013).

[45] O. Hosten, M. T. Rakher, J. T. Barreiro, N. A. Peters, and P. G. Kwiat. Counterfactual quantum computation through quantum interrogation. *Nature*, **439**, 949 (2006).

[46] W. P. Putnam and M. F. Yanik. Noninvasive electron microscopy with interaction-free quantum measurements. *Phys. Rev. A*, **80**, 040902 (2009).

[47] M. H. Anderson, J. R. Ensher, M. R. Matthews, C. E. Wieman, and E. A. Cornell. Observation of Bose-Einstein Condensation in a Dilute Atomic Vapor. *Science*, **269**, 198 (1995).

[48] K. B. Davis, M. O. Mewes, M. R. Andrews, N. J. van Druten, D. S. Durfee, D. M. Kurn, and W. Ketterle. Bose-Einstein Condensation in a Gas of Sodium Atoms. *Phys. Rev. Lett.*, **75**, 3969 (1995).

[49] D. M. Stamper-Kurn, M. R. Andrews, A. P. Chikkatur, S. Inouye, H.-J. Miesner, J. Stenger, and W. Ketterle. Optical Confinement of a Bose-Einstein Condensate. *Phys. Rev. Lett.*, **80**, 2027 (1998).

[50] Y. Kawaguchi and M. Ueda. Spinor Bose-Einstein condensates. *Phys. Rep.*, **520**, 253 (2012). Spinor Bose–Einstein condensates.

[51] D. M. Stamper-Kurn and M. Ueda. Spinor Bose gases: Symmetries, magnetism, and quantum dynamics. *Rev. Mod. Phys.*, **85**, 1191 (2013).

[52] O. Topić. *Resonante Spindynamik in Bose-Einstein-Kondensaten.* PhD thesis, Technische Informationsbibliothek und Universitätsbibliothek Hannover (2009).

[53] C. Klempt, O. Topic, G. Gebreyesus, M. Scherer, T. Henninger, P. Hyllus, W. Ertmer, L. Santos, and J. J. Arlt. Multiresonant Spinor Dynamics in a Bose-Einstein Condensate. *Phys. Rev. Lett.*, **103**, 195302 (2009).

[54] M. Scherer. *Nichtklassische Zustände in Spinor-Bose-Einstein-Kondensaten.* PhD thesis, Leibniz Universität Hannover (2012).

[55] B. Lücke. *Multi-particle entanglement in a spinor Bose-Einstein condensate for quantum-enhanced interferometry*. PhD thesis, Technische Informationsbibliothek und Universitätsbibliothek Hannover (2014).

[56] K. Huang. *Statistical Mechanics*. Wiley, New York (1987).

[57] T. W. B. Kibble. Topology of cosmic domains and strings. *J. Phys. A: Math. Gen.*, **9**, 1387 (1976).

[58] N. Turok and J. Zadrozny. Dynamical generation of baryons at the electroweak transition. *Phys. Rev. Lett.*, **65**, 2331 (1990).

[59] W. H. Zurek. Cosmological experiments in superfluid helium? *Nature*, **317**, 505 (1985).

[60] H. Saito, Y. Kawaguchi, and M. Ueda. Symmetry breaking in scalar, spinor, and rotating Bose-Einstein condensates. *Nucl. Phys. A*, **790**, 737c (2007).

[61] C. N. Weiler, T. W. Neely, D. R. Scherer, A. S. Bradley, M. J. Davis, and B. P. Anderson. Spontaneous vortices in the formation of Bose-Einstein condensates. *Nature*, **455**, 948 (2008).

[62] T.-L. Ho. Spinor Bose Condensates in Optical Traps. *Phys. Rev. Lett.*, **81**, 742 (1998).

[63] T. Ohmi and K. Machida. Bose-Einstein Condensation with Internal Degrees of Freedom in Alkali Atom Gases. *J. Phys. Soc. Jpn.*, **67**, 1822 (1998).

[64] M. Vengalattore, S. R. Leslie, J. Guzman, and D. M. Stamper-Kurn. Spontaneously Modulated Spin Textures in a Dipolar Spinor Bose-Einstein Condensate. *Phys. Rev. Lett.*, **100**, 170403 (2008).

[65] J. Javanainen and S. M. Yoo. Quantum Phase of a Bose-Einstein Condensate with an Arbitrary Number of Atoms. *Phys. Rev. Lett.*, **76**, 161 (1996).

[66] J. I. Cirac, C. W. Gardiner, M. Naraschewski, and P. Zoller. Continuous observation of interference fringes from Bose condensates. *Phys. Rev. A*, **54**, R3714 (1996).

[67] C. Klempt, O. Topic, G. Gebreyesus, M. Scherer, T. Henninger, P. Hyllus, W. Ertmer, L. Santos, and J. J. Arlt. Parametric Amplification of Vacuum Fluctuations in a Spinor Condensate. *Phys. Rev. Lett.*, **104**, 195303 (2010).

[68] L. E. Sadler, J. M. Higbie, S. R. Leslie, M. Vengalattore, and D. M. Stamper-Kurn. Spontaneous symmetry breaking in a quenched ferromagnetic spinor Bose-Einstein condensate. *Nature*, **443**, 312 (2006).

[69] J. J. . Bollinger, W. M. Itano, D. J. Wineland, and D. J. Heinzen. Optimal frequency measurements with maximally correlated states. *Phys. Rev. A*, **54**, R4649 (1996).

[70] M. J. Holland and K. Burnett. Interferometric detection of optical phase shifts at the Heisenberg limit. *Phys. Rev. Lett.*, **71**, 1355 (1993).

[71] G. Tóth, C. Knapp, O. Gühne, and H. J. Briegel. Optimal Spin Squeezing Inequalities Detect Bound Entanglement in Spin Models. *Phys. Rev. Lett.*, **99**, 250405 (2007).

[72] G. Vitagliano, I. Apellaniz, I. n. L. Egusquiza, and G. Tóth. Spin squeezing and entanglement for an arbitrary spin. *Phys. Rev. A*, **89**, 032307 (2014).

[73] T. Vanderbruggen, S. Bernon, A. Bertoldi, A. Landragin, and P. Bouyer. Spin-squeezing and Dicke-state preparation by heterodyne measurement. *Phys. Rev. A*, **83**, 013821 (2011).

[74] R. Bücker, J. Grond, S. Manz, T. Berrada, T. Betz, C. Koller, U. Hohenester, T. Schumm, A. Perrin, and J. Schmiedmayer. Twin-atom beams. *Nature Phys.*, **7**, 608 (2011).

[75] R. Krischek, C. Schwemmer, W. Wieczorek, H. Weinfurter, P. Hyllus, L. Pezzé, and A. Smerzi. Useful Multiparticle Entanglement and Sub-Shot-Noise Sensitivity in Experimental Phase Estimation. *Phys. Rev. Lett.*, **107**, 080504 (2011).

[76] G. Tóth. Multipartite entanglement and high-precision metrology. *Phys. Rev. A*, **85**, 022322 (2012).

[77] P. Hyllus, W. Laskowski, R. Krischek, C. Schwemmer, W. Wieczorek, H. Weinfurter, L. Pezzé, and A. Smerzi. Fisher information and multiparticle entanglement. *Phys. Rev. A*, **85**, 022321 (2012).

[78] N. Kiesel, C. Schmid, G. Tóth, E. Solano, and H. Weinfurter. Experimental Observation of Four-Photon Entangled Dicke State with High Fidelity. *Phys. Rev. Lett.*, **98**, 063604 (2007).

[79] W. Wieczorek, R. Krischek, N. Kiesel, P. Michelberger, G. Tóth, and H. Weinfurter. Experimental Entanglement of a Six-Photon Symmetric Dicke State. *Phys. Rev. Lett.*, **103**, 020504 (2009).

[80] C. D. Hamley, C. S. Gerving, T. M. Hoang, E. M. Bookjans, and M. S. Chapman. Spin-nematic squeezed vacuum in a quantum gas. *Nature Phys.*, **8**, 305 (2012).

[81] W. H. Furry. Note on the Quantum-Mechanical Theory of Measurement. *Phys. Rev.*, **49**, 393 (1936).

[82] G. C. Ghirardi, A. Rimini, and T. Weber. Unified dynamics for microscopic and macroscopic systems. *Phys. Rev. D*, **34**, 470 (1986).

[83] A. Bassi and G. Ghirardi. Dynamical reduction models. *Phys. Rep.*, **379**, 257 (2003).

[84] R. Penrose. Quantum computation, entanglement and state reduction. *Philos. Trans. R. Soc. London, Ser. A*, **356**, 1927 (1998).

[85] L. Diósi. Notes on certain Newton gravity mechanisms of wavefunction localization and decoherence. *J. Phys. A: Math. Theor.*, **40**, 2989 (2007).

[86] D. T. Pegg. Spontaneous emission and absorber theory. *Phys. Scr.*, **1997**, 106 (1997).

[87] J. Laurat, T. Coudreau, G. Keller, N. Treps, and C. Fabre. Effects of mode coupling on the generation of quadrature Einstein-Podolsky-Rosen entanglement in a type-II optical parametric oscillator below threshold. *Phys. Rev. A*, **71**, 022313 (2005).

[88] G. Keller, V. D'Auria, N. Treps, T. Coudreau, J. Laurat, and C. Fabre. Experimental demonstration offrequency-degenerate bright EPR beamswith a self-phase-locked OPO. *Opt. Express*, **16**, 9351 (2008).

[89] P.-A. Moreau, F. Devaux, and E. Lantz. Einstein-Podolsky-Rosen Paradox in Twin Images. *Phys. Rev. Lett.*, **113**, 160401 (2014).

[90] E. S. Gómez, G. Cañas, E. Acuña, W. A. T. Nogueira, and G. Lima. Non-Gaussian-state generation certified using the Einstein-Podolsky-Rosen-steering inequality. *Phys. Rev. A*, **91**, 013801 (2015).

[91] M. Edgar, D. Tasca, F. Izdebski, R. Warburton, J. Leach, M. Agnew, G. Buller, R. Boyd, and M. Padgett. Imaging high-dimensional spatial entanglement with a camera. *Nat. Commun.*, **3**, 984 (2012).

[92] C. Schori, J. L. Sørensen, and E. S. Polzik. Narrow-band frequency tunable light source of continuous quadrature entanglement. *Phys. Rev. A*, **66**, 033802 (2002).

[93] W. P. Bowen, N. Treps, R. Schnabel, and P. K. Lam. Experimental Demonstration of Continuous Variable Polarization Entanglement. *Phys. Rev. Lett.*, **89**, 253601 (2002).

[94] W. P. Bowen, R. Schnabel, P. K. Lam, and T. C. Ralph. Experimental Investigation of Criteria for Continuous Variable Entanglement. *Phys. Rev. Lett.*, **90**, 043601 (2003).

[95] K. Wagner, J. Janousek, V. Delaubert, H. Zou, C. Harb, N. Treps, J. F. Morizur, P. K. Lam, and H. A. Bachor. Entangling the Spatial Properties of Laser Beams. *Science*, **321**, 541 (2008).

[96] C. Silberhorn, P. K. Lam, O. Weiß, F. König, N. Korolkova, and G. Leuchs. Generation of Continuous Variable Einstein-Podolsky-Rosen Entanglement via the Kerr Nonlinearity in an Optical Fiber. *Phys. Rev. Lett.*, **86**, 4267 (2001).

[97] V. Boyer, A. M. Marino, R. C. Pooser, and P. D. Lett. Entangled Images from Four-Wave Mixing. *Science*, **321**, 544 (2008).

[98] O. Serot, N. Carjan, and D. Strottman. Transient behaviour in quantum tunneling: time-dependent approach to alpha decay. *Nucl. Phys. A*, **569**, 562 (1994).

[99] L. S. Schulman. Continuous and pulsed observations in the quantum Zeno effect. *Phys. Rev. A*, **57**, 1509 (1998).

[100] K. Koshino and A. Shimizu. Quantum Zeno effect by general measurements. *Phys. Rep.*, **412**, 191 (2005).

[101] C. Balzer, R. Huesmann, W. Neuhauser, and P. Toschek. The quantum Zeno effect - evolution of an atom impeded by measurement. *Opt. Commun.*, **180**, 115 (2000).

[102] C. Balzer, T. Hannemann, D. Reiß, C. Wunderlich, W. Neuhauser, and P. Toschek. A relaxationless demonstration of the Quantum Zeno paradox on an individual atom. *Opt. Commun.*, **211**, 235 (2002).

[103] B. Nagels, L. J. F. Hermans, and P. L. Chapovsky. Quantum Zeno Effect Induced by Collisions. *Phys. Rev. Lett.*, **79**, 3097 (1997).

[104] K. Mølhave and M. Drewsen. Demonstration of the continuous quantum zeno effect in optical pumping. *Phys. Lett. A*, **268**, 45 (2000).

[105] T. Nakanishi, K. Yamane, and M. Kitano. Absorption-free optical control of spin systems: The quantum Zeno effect in optical pumping. *Phys. Rev. A*, **65**, 013404 (2001).

[106] G. Barontini, R. Labouvie, F. Stubenrauch, A. Vogler, V. Guarrera, and H. Ott. Controlling the Dynamics of an Open Many-Body Quantum System with Localized Dissipation. *Phys. Rev. Lett.*, **110**, 035302 (2013).

[107] S. R. Wilkinson, C. F. Bharucha, M. C. Fischer, K. W. Madison, P. R. Morrow, Q. Niu, B. Sundaram, and M. G. Raizen. Experimental evidence for non-exponential decay in quantum tunnelling. *Nature*, **387**, 575 (1997).

[108] A. G. Kofman and G. Kurizki. Acceleration of quantum decay processes by frequent observations. *Nature*, **405**, 546 (2000).

[109] J. D. Franson, B. C. Jacobs, and T. B. Pittman. Quantum computing using single photons and the Zeno effect. *Phys. Rev. A*, **70**, 062302 (2004).

[110] P. Facchi, S. Tasaki, S. Pascazio, H. Nakazato, A. Tokuse, and D. A. Lidar. Control of decoherence: Analysis and comparison of three different strategies. *Phys. Rev. A*, **71**, 022302 (2005).

[111] M. Renninger. Messungen ohne Störung des Meßobjekts. *Z. Phys.*, **158**, 417 (1960).

[112] R. H. Dicke. Interaction-free quantum measurements: A paradox? *Am. J. Phys*, **49**, 925 (1981).

[113] C. K. Hong and L. Mandel. Experimental realization of a localized one-photon state. *Phys. Rev. Lett.*, **56**, 58 (1986).

[114] E. d. M. Van Voorthuysen. Realization of an interaction-free measurement of the presence of an object in a light beam. *Am. J. Phys*, **64**, 1504 (1996).

[115] M. Hafner and J. Summhammer. Experiment on interaction-free measurement in neutron interferometry. *Phys. Lett. A*, **235**, 563 (1997).

[116] A. G. White, J. R. Mitchell, O. Nairz, and P. G. Kwiat. "Interaction-free" imaging. *Phys. Rev. A*, **58**, 605 (1998).

[117] X.-s. Ma, X. Guo, C. Schuck, K. Y. Fong, L. Jiang, and H. X. Tang. On-chip interaction-free measurements via the quantum Zeno effect. *Phys. Rev. A*, **90**, 042109 (2014).

[118] G. Mitchison and R. Jozsa. Counterfactual computation. *P R SOC A*, **457**, 1175 (2001).

[119] A. Luis and J. Peřina. Zeno Effect in Parametric Down-Conversion. *Phys. Rev. Lett.*, **76**, 4340 (1996).

[120] D. Home and M. Whitaker. A Conceptual Analysis of Quantum Zeno; Paradox, Measurement, and Experiment. *Ann. Phys.*, **258**, 237 (1997).

[121] M. G. Paris. Displacement operator by beam splitter. *Phys. Lett. A*, **217**, 78 (1996).

[122] H. M. Wiseman, S. J. Jones, and A. C. Doherty. Steering, Entanglement, Nonlocality, and the Einstein-Podolsky-Rosen Paradox. *Phys. Rev. Lett.*, **98**, 140402 (2007).

[123] E. G. Cavalcanti, S. J. Jones, H. M. Wiseman, and M. D. Reid. Experimental criteria for steering and the Einstein-Podolsky-Rosen paradox. *Phys. Rev. A*, **80**, 032112 (2009).

[124] V. Händchen, T. Eberle, S. Steinlechner, A. Samblowski, T. Franz, R. F. Werner, and R. Schnabel. Observation of one-way Einstein-Podolsky-Rosen steering. *Nat. Photonics*, **6**, 596 (2012).

[125] R. Lopes, A. Imanaliev, A. Aspect, M. Cheneau, D. Boiron, and C. I. Westbrook. Atomic Hong-Ou-Mandel experiment. *Nature*, **520**, 66 (2015).

[126] L. Pezzé and A. Smerzi. Ultrasensitive Two-Mode Interferometry with Single-Mode Number Squeezing. *Phys. Rev. Lett.*, **110**, 163604 (2013).

Publications

[A1] M. Scherer, B. Lücke, J. Peise, O. Topic, G. Gebreyesus, F. Deuretzbacher, W. Ertmer, L. Santos, C. Klempt, and J. J. Arlt. Spontaneous symmetry breaking in spinor Bose-Einstein condensates *Phys. Rev. A*, **88**, 053624 (2013).
DOI: 10.1103/PhysRevA.88.053624

[A2] B. Lücke, M. Scherer, J. Kruse, L. Pezzé, F. Deuretzbacher, P. Hyllus, O. Topic, J. Peise, W. Ertmer, J. Arlt, L. Santos, A. Smerzi, and C. Klempt. Twin Matter Waves for Interferometry Beyond the Classical Limit *Science*, **334**, 773 (2011).
DOI: 10.1126/science.1208798

[A3] B. Lücke, J. Peise, G. Vitagliano, J. J. Arlt, L. Santos, G. Tóth, and C. Klempt. Detecting Multiparticle Entanglement of Dicke States *Phys. Rev. Lett.*, **112**, 155304 (2014). DOI: 10.1103/PhysRevLett.112.155304

[A4] I. Apellaniz, B. Lücke, J. Peise, C. Klempt, and G. Tóth. Detecting metrologically useful entanglement in the vicinity of Dicke states *New J. Phys.*, **17**, 083027 (2015). DOI: 10.1088/1367-2630/17/8/083027

[A5] J. Peise, I. Kruse, K. Lange, B. Lücke, L. Pezzé, J. Arlt, W. Ertmer, K. Hammerer, L. Santos, A. Smerzi, and C. Klempt. Satisfying the Einstein-Podolsky-Rosen criterion with massive particles *Nat. Commun.*, **6**, 8984 (2015).
DOI: 10.1038/ncomms9984

[A6] J. Peise, B. Lücke, L. Pezzé, F. Deuretzbacher, W. Ertmer, J. Arlt, A. Smerzi, L. Santos, and C. Klempt. Interaction-free measurements by quantum Zeno stabilization of ultracold atoms *Nat. Commun.*, **6**, 6811 (2015).
DOI: 10.1038/ncomms7811

Danksagung

Die präsentierten Ergebnisse entstanden in langjähriger Zusammenarbeit zahlreicher Teammitglieder, denen ich an dieser Stelle meinen herzlichen Dank aussprechen möchte. Zuallererst möchte ich meinem Doktorvater Prof. Wolfgang Ertmer danken für die Möglichkeit meine Doktorarbeit am Institut für Quantenoptik anzufertigen und für die Bereitstellung des exzellenten wissenschaftlichen Umfeldes.

Ganz besonders möchte ich mich bei PD. Carsten Klempt bedanken für das Vertrauen mich in seine Arbeitsgruppe aufzunehmen. Die regelmäßigen Diskussionen, sowie die tatkräftige Unterstützung bei Problemlösungen haben die Arbeit deutlich vorangebracht und mich in meiner Entwicklung stark gefördert.

Ein großer Dank geht an meine langjährigen Kollegen Manuel Scherer und Bernd Lücke, die mich in das bestehende Experiment eingearbeitet haben. Sie haben mich unzähligen experimentellen Feinheiten gelehrt, ohne deren Kenntnis ich im komplexen Experimentaufbau wohl verloren gewesen wäre. Auch die Zeit außerhalb des Labors hat mir viel Freude bereitet und die Promotion zu einem tollen Lebensabschnitt gemacht, den ich zu keinem Zeitpunkt bereut habe. Ebenso möchte ich mich bei meinen neueren Kollegen Ilka Kruse und Karsten Lange bedanken, die zum Abschluss meiner Arbeit Teil des Teams wurden und mich erwartungsvoll auf die nähere Zukunft des Experimentes blicken lassen.

Ebenfalls möchte ich mich bei unserem Masterand Sascha Kulas und Bacheloranden Henning Albers, Rouven Dreyer, David Roszak und Knut Stolzenberg bedanken mit denen ich gerne zusammen gearbeitet habe und die wichtige Projekte zum Experiment beigesteuert haben.

Ein sehr wichtiger Grundstein für die vergangenen, ertragreichen Jahre liegt in der engen Zusammenarbeit mit Arbeitsgruppen aus der Theorie. Hier ist Prof. Luis Santos vom Institut für theoretische Physik hervorzuheben, der unter anderem auch die Mentorenschaft für mich im Rahmen des RTG 1729 übernommen hat. Für die regelmäßigen und inspirierenden Diskussionen mit Prof. Luis Santos zusammen mit Frank Deuretzbacher möchte ich mich herzlich bedanken. Ebenso waren die ungezählten Diskussionen mit Augusto Smerzi und Luca Pezze in Florenz Ausgangspunkt für viele spannende Messkampagnen und die anschließenden Auswertung der aufgenommenen Daten ohne ihre Unterstützung nicht zu bewältigen. Gleichermaßen möchte ich mich bei Prof. Geza Toth in Bilbao bedanken. Des Weiteren möchte ich mich auch bei meinen Kollegen des Nachbar-Experiments bedanken. Insbesondere die langen Billardrunden nach Feierabend mit Jan Mahnke waren eine schöne Abwechslung zum Arbeitsalltag. Außerdem danke ich Georg Kleine Büning, Johannes Will, Stefan Jöllenbeck, Manuela Hanke, Richard Randoll, Andreas Hüper und Jiao Geng sowie den Arbeitsgruppen um Prof. Ernst Rasel, Prof. Silke und Prof. Christian Ospelkaus für die tolle Arbeitsatmosphäre, die das

Arbeiten in den vergangenen Jahren zu einer so schönen Zeit gemacht haben.

Vielen Dank an das Sekretariat, das den Ablauf am Institut so reibungsfrei ermöglicht und bei kleinen und größeren Problemen zur Seite steht. Zu nennen sind hier Gunhild Faber, Elke Hünitzsch, Birgit Ohlendorf, Barbara Thiele-Bode, Anne-Dore Göldner-Pauer, Natalie Koberstein und Katrin Pfennig.

Der größte Dank gilt meinen Eltern Elke und Dieter auf deren Unterstützung ich mich stets verlassen konnte und die mich so weit gebracht haben.

Vielen Dank euch allen!

Lebenslauf

Persönliche Daten

Name	Jan Christopher Peise
Geburtsdatum/-ort	21.05.1985 in Hannover, Deutschland

Promotionsstudium

seit 2010	Doktorarbeit am *Institut für Quantenoptik* der *Leibniz Universität Hannover*

Studium

07/2009 - 07/2010	Diplomarbeit am *Institut für Quantenoptik* der *Leibniz Universität Hannover* mit dem Thema "Methoden zur Untersuchung von Dekohärenz und Frequenzverschiebungen in ultrakalten Atomen"
2005-2010	Studium der Physik an der *Leibniz Universität Hannover*

Schulabschluss

2005	Abitur am *Gymnasium Langenhagen*